METHUEN'S MONOGRAPHS
ON PHYSICAL SUBJECTS

APPLICATIONS OF INTERFEROMETRY

W. EWART WILLIAMS

METHUEN'S MONOGRAPHS ON PHYSICAL SUBJECTS

General Editor: B. L. WORSNOP, B.Sc., Ph.D.
Headmaster of the Polytechnic School
and Special Lecturer in Radiology,
King's College, London

F'cap 8vo. Illustrated. Each 3s. net

THIS series is intended to supply readers of average scientific attainment with a compact statement of the modern position in each subject. The Honours student and the research worker in other branches of physics, those engaged on work in related sciences, and those who are no longer in contact with active scientific work, will find here a series of expositions by authors who are actively engaged in research on the subject of which they write.

For list of series, see back of this jacket

METHUEN & CO. LTD. LONDON

E. M. Forst.

Monographs on Physical Subjects

General Editor: B. L. Worsnop, B.Sc., Ph.D.

APPLICATIONS OF INTERFEROMETRY

METHUEN'S MONOGRAPHS ON PHYSICAL SUBJECTS

General Editor : B. L. WORSNOP, B.Sc., Ph.D.

3s. net

SPECTRA	R. C. JOHNSON
THE CONDUCTION OF ELECTRICITY THROUGH GASES	K. G. EMELÉUS
X-RAYS	B. L. WORSNOP
X-RAY CRYSTALLOGRAPHY	R. W. JAMES
THE COMMUTATOR MOTOR	F. J. TEAGO
APPLICATIONS OF INTERFEROMETRY	W. E. WILLIAMS
PHOTOCHEMISTRY	D. W. G. STYLE
THERMODYNAMICS	A. W. PORTER
ATMOSPHERIC ELECTRICITY	B. F. J. SCHONLAND
THE METHOD OF DIMENSIONS	A. W. PORTER
PHYSICAL CONSTANTS	W. H. J. CHILDS
THE KINETIC THEORY OF GASES	MARTIN KNUDSEN
RELATIVITY PHYSICS	W. H. MCCREA
MOLECULAR BEAMS	R. G. J. FRASER
COSMOLOGICAL THEORY	G. G. MCVITTIE
THE CYCLOTRON	W. B. MANN

3s. 6d. net

MAGNETISM	E. C. STONER
THERMIONIC VACUUM TUBES	E. V. APPLETON
COLLISION PROCESSES IN GASES	F. L. ARNOT
ELECTROMAGNETIC WAVES	F. W. G. WHITE
THE GENERAL PRINCIPLES OF QUANTUM THEORY	G. TEMPLE
LOW TEMPERATURE PHYSICS	L. C. JACKSON
HIGH VOLTAGE PHYSICS	L. JACOB
FINE STRUCTURE IN LINE SPECTRA AND NUCLEAR SPIN	S. TOLANSKY
INFRA-RED AND RAMAN SPECTRA	G. B. B. M. SUTHERLAND
THERMIONIC EMISSION	T. J. JONES
ELECTRON DIFFRACTION	R. BEECHING
MERCURY ARCS	F. J. TEAGO and J. F. GILL
AN INTRODUCTION TO VECTOR ANALYSIS FOR PHYSICISTS AND ENGINEERS	B. HAGUE
WIRELESS RECEIVERS	C. W. OATLEY

4s. net

WAVE MECHANICS	H. T. FLINT
THE EARTH'S MAGNETISM	S. CHAPMAN
ALTERNATING CURRENT MEASUREMENTS	D. OWEN
DIPOLE MOMENTS	R. J. W. LE FÈVRE
FLUORESCENCE AND PHOSPHORESCENCE	E. HIRSCHLAFF
THE PHYSICAL PRINCIPLES OF WIRELESS	J. A. RATCLIFFE

IN PREPARATION

SURFACE TENSION	ALLAN FERGUSON
ELECTRON OPTICS	N. LEVIN

APPLICATIONS OF INTERFEROMETRY

BY

W. EWART WILLIAMS, M.Sc.

LECTURER IN PHYSICS IN THE UNIVERSITY OF LONDON, KING'S COLLEGE

WITH A PREFACE BY

O. W. RICHARDSON, F.R.S.

YARROW RESEARCH PROFESSOR OF THE ROYAL SOCIETY
NOBEL LAUREATE IN PHYSICS, 1929

WITH 43 DIAGRAMS

SECOND EDITION

METHUEN & CO. LTD.
36 ESSEX STREET W.C.
LONDON

First Published . . *October 9th 1930*
Second Edition . . . *1941*

PRINTED IN GREAT BRITAIN

GENERAL PREFACE

THIS series of small monographs is one which should commend itself to a wide field of readers.

The reader will find in these volumes an up-to-date résumé of the developments in the subjects considered. The references to the standard works and to recent papers will enable him to pursue further those subjects which he finds of especial interest. The monographs should therefore be of great service to physics students who have examinations to consider, to those who are engaged in research in other branches of physics and allied sciences, and to the large number of science masters and others interested in the development of physical science who are no longer in close contact with recent work.

From a consideration of the list of authors it is clear that the reader need have no doubt of the accuracy of the general accounts found in these volumes.

O. W. RICHARDSON

KING'S COLLEGE
June, 1928

PREFACE

ALTHOUGH this work is primarily intended for the University student, it is hoped that the various technical applications described in it will make it of some value to chemists and engineers who are making increasing use of Interference methods and apparatus in their respective professions.

The subject is so wide that it has been necessary to omit all mention of Stationary waves and Infra-red Interferometry. Other sections have had to be curtailed, but the references given at the end of each chapter will form a supplement.

Michelson's Stellar Interferometer has been dealt with at some length, not only on account of its importance, but also because the exact action of the Interferometer (as distinguished from the earlier double slit method) is apparently not generally understood.

I am especially indebted to Dr. G. Hansen for a copy of the curves given in Fig. 6.8. These have made it possible to derive simple expressions for the Resolving Power of Lummer Plates under actual working conditions, instead of for the hypothetical case of grazing emergence.

Finally, I also wish to thank Messrs. A. Hilger Ltd. for the loan of the blocks of Figs. 2.4 and 2.5, and Messrs. Carl Zeiss for the blocks of Figs. 2.6 and 5.6.

W. E. W.

KING'S COLLEGE
STRAND, W.C.2
May, 1930

CONTENTS

CHAP.		PAGE
I	Introductory	1
II	Interferometer Arrangements involving Point or Line Sources (Division of Wavefront)	6
III	Interferometer Arrangements involving a Division of Amplitude . . .	32
IV	The Michelson Interferometer and its Applications	46
V	Simultaneous Division of Amplitude and of Wavefront	63
VI	Interference Effects with more than two Beams	76

SUBJECT INDEX

Adjustment of Jamin Interferometer, 43
— of Michelson Interferometer, 70

Benoit, Fabry and Perot's Determination of the Metre, 89
Brewster's Fringes, 41

Channelled Spectra, 101

Diffraction Grating, 23

Earth Rotation Experiment, 61
Echelon (Reflection), 28
Edser & Butler Bands, 101
Elastic Constants by Interference Methods, 37
Exact Factions Method, 83

Fabry and Perot Interferometer, 76
— — — Resolving Power, 77
— — — Wavelength Measurement, 82
— — — Two or more in series, 91
Fizeau Interferoscope, 64

Gauge Testing by Interferometry, 38
Gerhardt Microscope Interferometer, 23
Gratings, Diffraction, 23
— — Echelon, 27

Haidinger's Fringes, 33
Herschel Fringes, 40

Jamin Interferometer, 42

Kennedy Half Shade Method, 59
Kösters' Comparator, 74

Lens, Interferometer, 65
Lummer Plate, 94

Mascart and Jamin Interferometer, 57
Michelson Metre Determination, 51
— Interferometer, 46
— Stellar Interferometer, 16
Michelson and Morley Experiment, 58

Newton's Rings, 34

Phase change, 34, 87
Poisson's Ratio by Interference Method, 37

Rayleigh Refractometer, 8
Resolving Power, Diffraction Grating, 27
— — Echelon, 28
— — Fabry Perot, 78
— — Lummer Plate, 97

Screw testing, 88
Soap film thickness, 49
Superposition Fringes, 88
Stellar Interferometer, 16

Twyman and Green Interferometer, 65

Visibility of Fringes, 49

White Light Fringes, 48

APPLICATIONS OF INTERFEROMETRY

CHAPTER I

INTRODUCTORY

THE fundamental basis of the phenomenon of Light Interference is the Principle of Superposition due to Thomas Young. Suppose that due to a single wave train we have a displacement X in a given direction at a certain point and time and that another train acting by itself have a corresponding displacement Y, the principle states that the *instantaneous* resultant displacement of the two waves acting together is the algebraic sum of the separate displacements.

$$R = X + Y.$$

This additive principle which is only approximately valid for vibrations in matter must hold exactly for light vibrations since practically the whole of Optics is based on its correctness. Although not understood at the time, it is tacitly included in Huyghens' method of constructing the new position of a wavefront as the envelope of secondary wavelets. In one sense the term Interference is a misnomer, for, as Young himself realized, this principle of superposition implies the absolute independence of the individual components of the resultant displacement. This is in accordance with the experiments of Ebert which showed that one light beam however intense had no effect on another beam crossing its path.

The field of 'Interference' of Light is so wide that it has become customary to divide it into two parts. The study of the interference effects due to particular shapes of wavefronts is termed *Diffraction*, and the term *Interference* is limited to mean the effect of combining two or more separate beams that originally must have come from the same source.

When two or more beams 'interfere' to form the familiar fringe effect either we have a redistribution of the light, the bright parts collecting the energy from the darker portions, or a complementary pattern is formed elsewhere the bright parts of which correspond to the dark portions of the observed pattern. Fresnel's Biprism, the Diffraction Grating and the Lummer Plate are examples of cases giving an actual redistribution of the light in the field of view, while in Newton's Rings and the Michelson and Fabry-Perot Interferometers complementary patterns are formed.

Laws Governing the Interference of Light

Interference effects are only obtained if the interfering beams originate at a common source.

This law is a practical consequence of the enormously high frequency (of the order of 10^{15} per sec.) of visible light and the lack of homogeneity of known sources. Experiments indicate that the most nearly monochromatic light sources only radiate an unbroken train of waves for about 10^{-8} secs. After that interval another train will be started bearing no definite phase relationship with the first. If it were possible to photograph with an exposure time of this order or less, in all probability fringes could be obtained from separate sources. Again with a sufficiently short time of exposure we should be able to obtain interference effects between beams of different wavelengths or frequencies, as these effects are obtained with the longer electromagnetic or wireless waves, which are inherently similar. Practically, in consequence of the comparatively long period required to register the effects, the interfering sources must be

identical in all respects and this is only possible when the beams originate from a common source.

When the original beam has been plane polarized and is passed through a doubly refracting medium, we have the additional limitation (first given by Fresnel and Arago) that the vibrations must be analysed on a common azimuth before the interference effects are observable. This follows since the transverse vibrations of the two beams emerging from the doubly refracting medium are mutually perpendicular.

Classification of Interference Phenomena

We can divide the methods of obtaining Interference effects into two broad classes.

[A] Methods which require a point source, or if the interference effects are only required in one direction a line source (Division of Wavefront).

[B] Methods in which the beam is divided by partial reflection into two or more beams (Division of Amplitude).

In the first class, provided the point or line source is sufficiently fine, it is possible to have wavefronts with similar phases emerging in slightly different directions from the source. These can be further separated by mirrors, prisms and lenses and eventually brought together again to produce interference bands. The greater the area over which the wavefront must be of the same phase, or coherent, the smaller must be the angle the source subtends at the wavefront. Examples of this class are the Fresnel Biprism and Mirrors, Lloyd's mirror, Billet split lens, and Rayleigh Interferometer. When the slit is too wide the fringes disappear. This disappearance of the fringes was actually used by Michelson in his method of measuring the angular diameter of stars and by Gerhardt in his adaptation of Michelson's method to obtain the diameters of ultra-microscopic particles (see Chap. II, page 22). All diffraction gratings, including echelons, also belong to this class.

In the second class, where the beam is divided by partial reflection at a half silvered mirror, there is a

point to point correspondence between the wavefronts of the transmitted and reflected beams. Any peculiarities in the one are also present in the other. It therefore follows that however complex the original wavefront may be, the clearness of the interference effects is not impaired. This means that with division of amplitude, extended light sources may be used, so that in general the effects are much brighter. Examples of this class are the interference effects of thin films and the interferometer systems of Jamin, Mach, Michelson, Fabry Perot, and Lummer Gehrcke.

An interferometer of this second class can in special instances be modified and used as an instrument of the former class. It thereby gains many additional qualities and behaves in an entirely different way. A notable example of this is the modification by Twyman and Green of the Michelson interferometer.

Michelson in his book *Light Waves and their Uses* restricted the term Interferometer to denote any arrangement which separates a beam of light into two parts and allows them to reunite under conditions to produce interference. Common usage has however extended this definition to include all methods that divide the beam into any number of parts that are subsequently brought together to cause interference. For this reason it is convenient to subdivide each of the above classes according to whether we have two or more interfering beams. All the arrangements in Class A with the exception of Diffraction (including Echelon) Gratings belong to the double beam type, while the Fabry Perot and Lummer Gehrcke Interferometers of Class B are examples of the multiple beam type.

The applications of interference methods are so numerous that it would be impossible to include all in a book of this compass. Representative examples chosen for interest and importance are therefore considered, while many further applications will occur to the reader once the possibilities of any particular type are realized. The purely scientific or academic use of

an arrangement will be considered first and its technical applications afterwards. The simpler and better known interference methods will only be very briefly discussed in order to leave more space for the more complicated and lesser-known arrangements.

GENERAL REFERENCES ON INTERFERENCE

Houston : *Treatise on Light*, Chapter 9 (Longmans).
Preston : *Theory of Light* (5th Edition), Chapter I, Sect. III, Chapter II (Macmillan).
Schuster : *Theory of Optics*, Chapters I–IV (Arnold).
Wood : *Physical Optics*, Chapter VI (Macmillan).
Bouasse and Carrière : *Interférences* (Delagrave, Paris).
Fabry : *Applications des Interférences Lumineuses* (Paris).
Michelson : *Light Waves and their Uses* (out of print).
Michelson : *Studies in Optics* (Univ. of Chicago Press).
Gehrcke : *Die Anwendung der Interferenzen* (out of print).

CHAPTER II

INTERFEROMETER ARRANGEMENTS INVOLVING POINT OR LINE SOURCES (DIVISION OF WAVEFRONT)

THE first type of Interferometer, namely that by means of which Young verified the principle of the interference of light, was of this class. A primary slit limits the light to a cylindrical wavefront, and two parts of this wavefront are selected by two further slits. These in turn are equivalent to two secondary sources according to Huyghens' theory, and because they have corresponding phases (having come originally from the single narrow primary slit) wherever the beams from the second slits overlap, interference fringes are obtained. Young's fringes can be observed either in the neighbourhood of the double slit or with a telescope focussed for infinity if a sufficiently strong source is available.

Instead of forming the two secondary sources by means of slits, two sources, either images of a common source, or a real source and its image, may be used. This can be effected in various ways such as the Fresnel Inclined Mirrors or Biprism, the Single Mirror of Lloyd or the split lens method of Billet.

It is of interest to see in a general way why such narrow sources are essential. A and B (Fig. 2.1) are the source and image or two images of the same source produced by any of the above arrangements and S is a screen (or the focal plane of a low power microscope), distant D from 0 the midpoint of AB. Whether there is a bright or a dark fringe at any point P distant x

from N (ON $\perp^{ar.}$ to S) depends on whether AP − BP is equal to an even or odd number of half wavelengths (assuming A and B are in phase with each other). Writing $2d$ for the distance AB, $AP - BP = \frac{2xd}{D}$ provided D is large compared with d. Let us suppose that for a particular value of x, say x_1, we have a bright fringe so that $\frac{2x_1d}{D} = m\lambda$, where λ is the wavelength and m an integer : $x_1 = \frac{m\lambda D}{2d}$.

If the two sources A and B (still in phase) are displaced downwards a distance z (i.e. $AA_1 = BB_1 = z$) the value of x *as measured* from *the old origin* N for the same bright fringe will be $\frac{m\lambda D}{2d} + z$ since the same fringe has been moved down from P to P′ a distance z. If PP′ happens to be equal to the distance between successive fringes, i.e. $= \frac{\lambda D}{2d}$, then all traces of interference bands would be obliterated if the sources at A and B had a width equal to $\frac{\lambda D}{2d}$. To obtain clear distinct fringes the slit source should not be wider than about a quarter of this value. This constitutes a real disadvantage in this type of interferometer ; if it is to be used with monochromatic light, only a few sources can be obtained of sufficient intensity. A coal gas-oxygen blow lamp playing on a hard glass rod furnishes a clean and steady source of sufficient intensity for extended measurements for the sodium lines. A quartz mercury

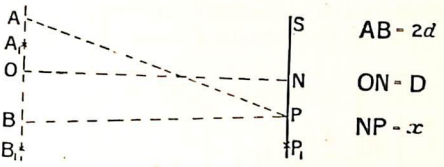

FIG. 2.1.—Interference between two point sources

lamp is also suitable if the fringes are observed with a Wratten filter, but the path difference between the beams can never be very high.

The Rayleigh Interferometer

This instrument was devised by Rayleigh [1] to determine the refractive indices of the newly discovered gases Argon and Helium. Subsequently it has been considerably developed by Haber, Löwe, Zeiss, Hilger and others. Essentially it is a diffraction grating with two slits, although, as in the case of the usual diffraction grating, it is not the diffraction effects at each slit or ruling that give it its important properties, but the *interference effects* of the beams diffracted at the several apertures.

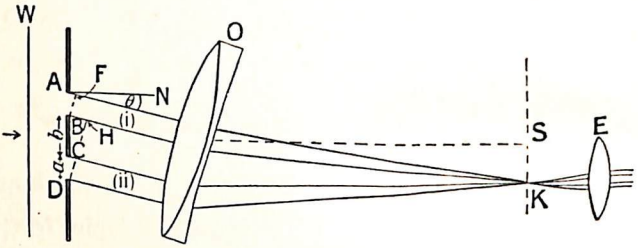

Fig. 2.2.—Interference between two sections of a plane wavefront

If a plane wavefront W (Fig. 2.2) emerging from a collimator falls normally on a diaphragm with two slits of width 'a', separated by a distance 'b', any one aperture such as AB may be considered as a plane wavefront source. If A is the total amplitude due to a single slit in the normal direction AN, the amplitude in a direction θ is given by $A \sin\left(\frac{\pi a \sin\theta}{\lambda}\right) \Big/ \left(\frac{\pi a \sin\theta}{\lambda}\right)$.

When a is large compared with λ as in this case, we are only concerned with small values of θ and the angle can be substituted for its sine.

If we have two trains of waves represented by $y_1 = r \sin \omega t$ and $y_2 = r \sin(\omega t + \Delta)$, where Δ is the phase

difference between them, the resultant displacement is by Young's principle of superposition $y = y_1 + y_2$.

This gives

$$y = r\{\sin \omega t + \sin(\omega t + \Delta)\} = 2r \cos \frac{\Delta}{2} \sin(\omega t + \delta)$$

where $\tan \delta = \dfrac{\sin \Delta}{1 + \cos \Delta}$. The amplitude of the resultant train is $2r \cos \dfrac{\Delta}{2}$ and the intensity $4r^2 \cos^2 \dfrac{\Delta}{2}$.

Applying it to the case under consideration, the path difference between corresponding parts of (i) and (ii) is $BH = (a + b)\ \theta$ so that the phase difference Δ is consequently $\dfrac{2\pi}{\lambda}(a + b)\ \theta$.

The expression for the resultant intensity in any direction θ is therefore :—

$$4A^2 \frac{\sin^2\left(\dfrac{\pi a \theta}{\lambda}\right)}{\left(\dfrac{\pi a \theta}{\lambda}\right)^2} \cdot \cos^2\left(\frac{\pi\ (a + b)\ \theta}{\lambda}\right). \qquad (1)$$

If 'a' is considerably smaller than 'b' the cosine term varies more rapidly with θ than the sine term. The cosine term has maximum values of unity when $\theta = 0, \dfrac{\lambda}{(a + b)}, \dfrac{2\lambda}{(a + b)}$, etc., the angle between the bright fringes being $\dfrac{\lambda}{(a + b)}$; the other factor which can be regarded as the envelope of the cosine term has maxima when $\theta = 0, \dfrac{1{\cdot}43\lambda}{a}$, and minima when $\theta = \dfrac{\lambda}{a}, \dfrac{2\lambda}{a}$, etc. These are shown in Fig. 2.3 where the dotted curve A refers to $\sin^2\left(\dfrac{\pi a \theta}{\lambda}\right) \Big/ \left(\dfrac{\pi a \theta}{\lambda}\right)^2$ and the solid curve B the $\cos^2\left(\dfrac{\pi\ (a + b)\ \theta}{\lambda}\right)$ term. The solid curve

of Fig. 2.3 represents the intensity at the focal plane SK of the telescope OE in Fig. 2.2, the point s of this figure corresponding to 0 in Fig. 2.3. It is important to note that the intensity curve of any particular fringe is practically a $\cos^2 \alpha$ curve.

When the light source is heterogeneous only the central fringe will be clearly defined. If white light is used, for example, the central fringe is white, while the fringes on either side are coloured, this effect becoming more and more pronounced away from the centre until, after five or six fringes on either side, no more can be seen. The fringes are red on the side away from the centre and violet on the inside. This follows since the angle between the fringes is proportional to the wave-length.

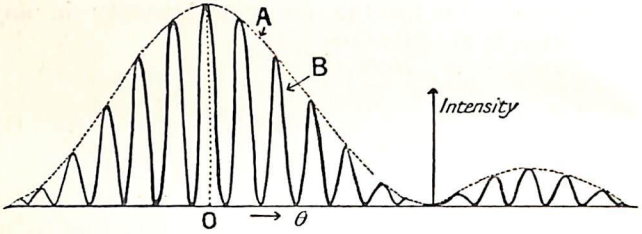

FIG. 2.3.—Intensity curve for double slit arrangement

If now a thin plate of refractive index μ and thickness t is placed in front of one aperture, e.g. AB in Fig. 2.2, a path difference $(\mu - 1)\ t$ is introduced, and the fringe system is displaced. If $(\mu - 1)\ t$ is small, say three or four wavelengths, the central white band is displaced to the position previously occupied by the third or fourth coloured fringe. The practical method of employing this principle is shown in the modern forms of Rayleigh's instrument as made by A. Hilger and C. Zeiss.

The plan of the upper half is shown in Fig. 2.4 ; the light from a narrow vertical slit A is collimated by an achromatic objective B, in front of which are two vertical slit apertures about 4 mms. wide and 12 mms.

apart. The two parallel beams after passing through the gas chambers D and E pass through two thin glass plates inclined at about 45° to the beam. One plate K is fixed, while the other L can be rotated on a horizontal axis perpendicular to the incident light. The interference bands are observed by the telescope QR. As the slits are widely separated, the fringes are very close, and need an extremely high power eyepiece for convenient observation. This high power is only needed in the horizontal plane, so that a great saving of light is effected by using as the eyepiece a cylinder of glass 1–2 mms. diameter, with its axis parallel to the slits A and C.

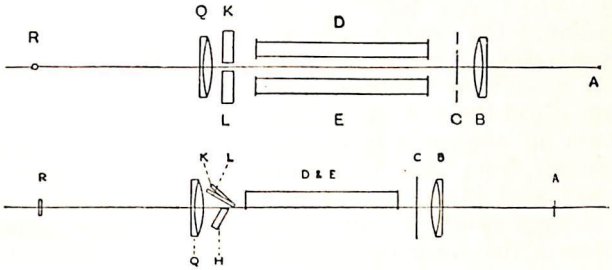

FIGS. 2.4 and 2.5.—Plan and Side Elevation of Rayleigh Refractometer

The side view is shown in Fig. 2.5: immediately below L and K is a parallel plate that extends across both beams in the lower half. Its purpose is to lift the lower beam so that a sharp separating line is obtained between the upper and lower set of fringes which forms a fiduciary system.

The movable plate L is controlled by an 8-inch arm which has a hardened polished steel end. A spring plunger keeps this end in contact with a micrometer screw carrying a divided drum; the thickness of the plate L is chosen so that one division on the drum represents a shift of less than $\frac{1}{10}$ of the distance between the bands.

The Rayleigh Interferometer can be used either to

determine the refractive index of a gas or a liquid or to determine the percentage of impurity in a mixture. The drum is first calibrated using a monochromatic light source at different points along its range. This means finding the mean drum rotation for a displacement of one fringe. Substituting white light the position of the drum is found where the white light fringes in the two halves of the field of view coincide. This gives the zero reading of the instrument. The unknown gas or liquid is then passed into one chamber and the white light fringes are brought into coincidence again. The new drum reading gives the optical path difference $(\mu_A - \mu_B)\ l$ as a total number n wavelengths plus a fraction. The wavelength will be approximately a mean value for white light, about ·55 to ·57 μ.

It sometimes happens that when a comparatively large tilt of the plate has to be made, and the dispersive power of the substance under examination is very different from that of the tilted plate, difficulty is experienced in deciding which band of the upper set of fringes most closely resembles the white central fringe in the lower half. Under these circumstances a preliminary measurement must be made. With gases, readings may be obtained at intermediate pressures, or at intermediate concentrations with liquids, or alternatively shorter chambers can be used.

For work of highest accuracy it is necessary to use monochromatic sources. This is so even when no doubt exists as to which is the central fringe, since the energy distribution in the upper fringe is slightly different from that in the lower half, due to the difference in dispersion of the glass plate and the substance. It is equivalent to a change in the effective wavelength of the white light source. The error is eliminated by using a white light source to locate the correct fringe and substituting a monochromatic source to obtain the fractional part accurately. (It will be realized that when a monochromatic source is used it is impossible to differentiate between one fringe and another.)

The problem of calibration of a Rayleigh Refractometer has been discussed by Edwards [2] and Adams,[3] who have also considered the errors due to dispersion.

Messrs. Carl Zeiss also manufacture a portable type which is based on the auto-collimating principle. It is shown diagrammatically in Fig. 2.6 which gives the plan and side elevation. The light source (a small electric lamp) is focussed by a lens on a short slit, the beam being twice reflected by a suitable prism. It emerges from the objective, passes through the compensating and tilting plates, and gas chambers to a plane mirror S, in front of which is the double slit diaphragm. The light returns almost but not exactly on its own path, and the fringes are observed with the cylindrical glass rod Ok.

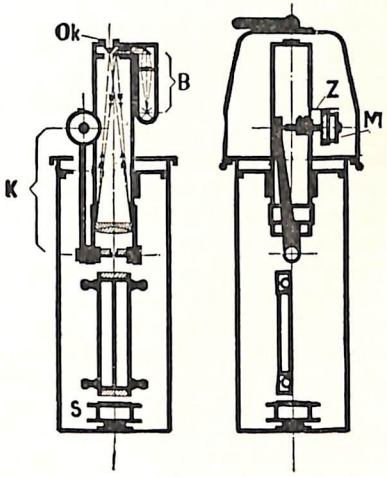

FIG. 2.6.—Zeiss Portable Rayleigh Refractometer

This form has the advantage that chambers of only half the length of those used in the standard form are needed to obtain the same sensitiveness, since the light traverses the gas or liquid columns twice. This is of importance since, with the reduced bulk, temperature control becomes easier. In the event of an accidental displacement of the mirror, this form is somewhat difficult to readjust.

The Rayleigh Refractometer is by far the most accurate and convenient means available of measuring small changes of refractive index. It surpasses other interferential methods such as the Jamin because the

fiduciary system is a similar set of fringes and not a cross wire. This feature was introduced by Haber and Löwe.[4] It will be obvious that readings with this arrangement will not be affected by a distortion of the framework or a displacement of the double slit, since both sets of bands are displaced equally. The chief advantage is, that with a similar set of fringes in the upper and lower half of the field separated by a very fine dividing line, the two sets can be placed in coincidence to a far greater precision than a cross wire could be set on the centre of a fringe. This is borne out in experiments with the coincidence type of range finder where alignment settings can be made with practice to a far greater accuracy than would be expected from considerations of the resolving power and magnification of the system. Since we are dealing with two virtual sources, the fringes are $\cos^2 \theta$ type, the intensity curves have a somewhat flat top (as compared with Fabry Perot fringes) decreasing slowly to zero on either side, and therefore a setting of a cross wire to within a tenth of the distance between the bands would be good. On the other hand, with the coincidence method a consistency of about $\frac{1}{40}$ is obtained after a little practice.

If l is the length of chamber and $\delta\mu$ the smallest change of index discernible,

$$\delta\mu \times l = \tfrac{1}{40} \times \lambda.$$

With 100 cm. gas chambers and $\lambda = 5461 \times 10^{-8}$ cm., $\delta\mu = 1 \times 10^{-8}$, which represents the order of the minimum change that can be observed. With 1 cm. chambers it is one unit in the sixth decimal place and so on in proportion. The total range of path difference that can be compensated for by tilting the plate is small. In the laboratory model of Zeiss it is about ·005 cm. or roughly 100 wavelengths and in the Hilger model 30 wavelengths. Thus the maximum difference of index $\Delta\mu$ that can be measured multiplied by the length of chambers must not exceed ·005 cm., but $\frac{\Delta\mu}{\delta\mu}$ is approximately 5000.

Theoretically, by employing sufficiently long columns the smallest change of index can be made measurable. Practically, however, this is limited by variations in index due to temperature which can only be made uniform between limits. For example, when 10 cm. chambers are used in a portable type (optical path 20 cm.) the fringes are not sufficiently steady for accurate setting until nearly an hour has elapsed after placing the liquids in the chambers, in spite of a very efficient shielding system. Thus while 100 cm. chambers can be used for gases, ·1 to 5 cm. is the greatest convenient length for liquids. When the index difference is large, the chamber length must be proportionately small.

The Rayleigh Refractometer is widely used in an ever increasing number of varied applications. Its accuracy is so high, that even with the permanent gases, the refractive indices of which are comparatively close, a displacement of $\frac{1}{10}$ of a fringe with 100 cm. chambers will occur when ·01 per cent. of Hydrogen is present as an impurity in air. A similar displacement would be given by ·006 per cent. of Helium, ·0045 per cent. of Sulphuretted Hydrogen, ·03 per cent. Carbon monoxide and ·0095 per cent. Carbon dioxide.

Technical applications of the above facts have been made in using the instrument for testing the permeability of balloon fabrics to hydrogen[5] and the quantitative analysis of flue gases[6] (CO, CO_2, SO_2 etc.).

The same type of interferometer using shorter cells for liquids can be used for estimating the salinity of seawater[7] and the concentration of salt solutions; although the difference in refractive index of solution of sodium and potassium chloride of similar concentration is very small, it is possible to use this instrument to determine the percentage in a mixture to a higher degree of accuracy than can be attained by careful and laborious chemical analysis. It is sufficiently sensitive to be used to check the stability of N/10 and N/100 solutions.

The instrument is widely used in Biochemical work

mainly because of the quantitative method of interferometry developed by Hirsch in the application of the Abderhalden reaction. These are described in Hirch's monograph *Fermentstudien* (Jena, 1917) and by Hirsch and Hecker.[8] A single example may be quoted; in testing the blood sera of children when only small quantities of liquid are available a special 1 mm. chamber has been employed. Even then the accuracy obtained is three or four times greater than with a total reflection refractometer.

The above list of applications would not be complete without reference to the Fire-damp tester of Beyling, Haber and Löwe.[9] Essentially it is a portable type as in Fig. 2.6, but is made in a flat shape so that it can be conveniently strapped to the observer. Two small accumulators are enclosed together with tubes of calcium chloride and soda lime. The zero position is found on the surface after filling both chambers with pure air. The standard chamber is then plugged with cotton-wool. To test the air in the mine, the polluted air is drawn into one vessel by means of a small rubber pressure ball, the cotton-wool being momentarily removed from the other side (to equalize pressure). The displacement of the white light fringes is compensated for by turning the drum which is graduated directly in percentage of methane and an accuracy of ·1 per cent. is obtained.

Michelson's Method of Measuring Stellar Diameters[10]

At the beginning of the chapter it was shown in a general way why narrow line or point sources are necessary for interference effects obtained by the method of division of wavefront. Another way of regarding it is that, for this method, the wavefront or light disturbance emerging from one aperture AB in Fig. 2.2 must be substantially the same (in phase and amplitude) as that emerging from the other aperture CD. This condition is only satisfied when the source either actually or virtually subtends a very small angle at the apertures.

Let A (Fig. 2.7) be a point source sufficiently distant from the telescope objective E that its image is formed at O in the focal plane F. If two parallel slits C and D (separation a) are placed in front of the telescope we get a fringe system at the focal plane, with O as the central bright band of zero path difference. The next bright fringe will occur at O′ where $CO' - DO' = \lambda$, and the angle ONO′ (α) between consecutive fringes is $\left(\frac{\lambda}{a}\right)$. With two virtual sources C and D, the intensity distribution of the bands is of the $\cos^2\theta$ type. The solid curve on the right of F gives the intensity dis-

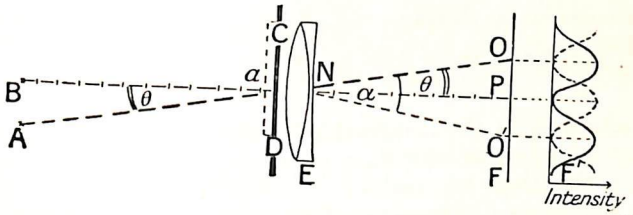

FIG. 2.7.—Fringes from two point sources with a double slit

tribution along F due to this point source. Another separate point source B will have a similar set of fringes with its centre (zero order) fringe P displaced through an angle θ relative to that of A when θ is the angle ANB. If the dotted line curve on the right represents the intensity distribution due to B, the fringes disappear when P is midway between O and O′, since in this position the two sets of fringes are complementary and give uniform intensity over F. Then

$$\theta = \tfrac{1}{2}\alpha = \frac{\lambda}{2a}.$$

Similarly the resultant fringe effect will vanish when the fringes of B are displaced 1·5 and 2·5 fringes from those of A, so that

$$\theta = \frac{3\lambda}{2a} \text{ or } \frac{5\lambda}{2a}.$$

Consider AB now to be a *line* object of uniform brightness: each point source on the line would have its own set of interference fringes and the eye observes the sum of their intensities. If the solid curve A′C (Fig. 2.8) is the Intensity distribution for the point A of Fig. 2.7, and the broken curves up to B′ the corresponding fringes for points along AB (Fig. 2.7), the resultant intensity curve will be DE. It will be clear that unless A′B′ extends to C there will be variations in the resultant intensity curve that the eye will interpret as faint interference bands. When A′B′= A′C the fringe separation, or a multiple of it, the field is uniformly illuminated. That is, the fringes disappear for a uniform *line* source when

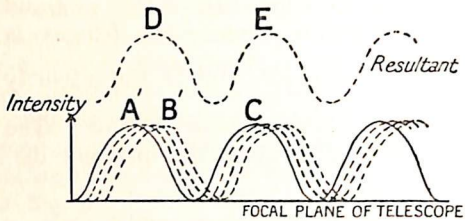

FIG. 2.8.—Fringes from an extended line source

$$\theta = \alpha,\ 2\alpha \text{ etc. } = \frac{\lambda}{a},\ \frac{2\lambda}{a}.$$

If AB in Fig. 2.7 represents a uniform *disc* its centre portions will contribute more light than the outer edges. The first disappearance of the fringes now occurs when

$$\theta = 1{\cdot}22\ \frac{\lambda}{a},$$

the 1·22 factor being derived in the same way as in the expression for the resolving power of a telescope of circular aperture.

The method was originally suggested by Fizeau [11] and a practical attempt was made by Stefan.[12] With the telescope apertures available, the disappearance of the fringes could not be obtained, since the fixed stars subtend far too small an angle. Michelson [10] however succeeded in applying the method to the moons of

Jupiter which subtend an angle of about one second of arc. Hamy[13] repeating the work used wider slits so that the fringes had greater intensity.

This method, in which the separation of the slits is adjusted until the fringes disappear, has only twice the sensitiveness of the open telescope. The fixed stars probably subtend angles of the order of ·01″ or less, so that impossibly large telescopes of 20–40 feet aperture would be required. In addition, the fringes would then be so fine and close together that an enormous magnification would be needed to render them visible.

Michelson's Stellar Interferometer

These factors led Michelson[14] to think of the idea of having as his effective apertures two mirrors M_1 and M_4 (Fig. 2.9) mounted on a long girder in front of the

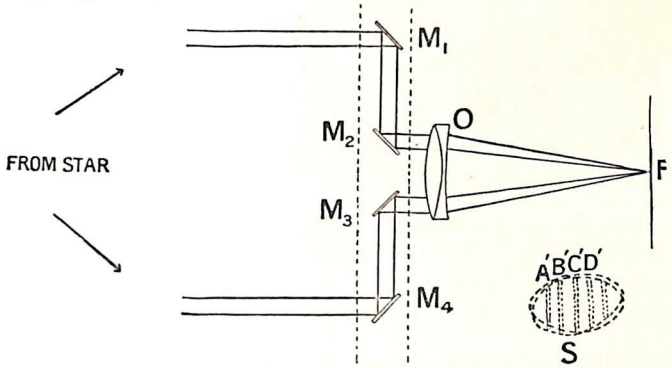

Fig. 2.9.—Michelson's Stellar Interferometer

telescope. These reflect the light to the inner mirrors $M_2 M_3$ which pass the beams into the telescope O. When the mirrors are adjusted ($M_1 \parallel$ to M_2 etc.) so that the beams overlap at the focal plane F the diffractional star disc image S (much enlarged because of the reduced aperture of the telescope) is crossed by a number of fine fringes A′B′C′D′. The outer mirrors $M_1 M_4$ are then moved symmetrically in or out until the fringes

disappear. If b is the smallest separation of $M_1 M_4$ that makes the fringes disappear, then

$$\theta \text{ (angle subtended by the star)} = 1{\cdot}22\,\frac{\lambda}{b} \text{ radians.}$$

For a disc of uniform brightness the fringes again disappear when the separation is $2b$, $3b$, etc. The effective wavelength λ should be determined by the same observer since it depends not only on the energy distribution of the star, but also on the Visual Acuity curve of the observer. [This can be obtained by measuring the angular fringe width of fringes from a close double slit (so that the star is effectively a point source), if the angular fringe width is β for a slit separation s, $\lambda = \beta s$.]

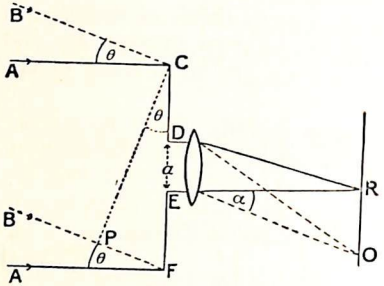

FIG. 2.10.—Magnification Effect obtained by Michelson's Method

The action of this type of interferometer can be understood from Fig. 2.10. Let the light from the end point A of a distant line source AB fall normally on the interferometer whose outer mirrors are C and F. If R is the zero order interference fringe due to A and O the first order fringe, DO — EO = λ, and the angle α between the fringes is as before $\frac{\lambda}{a}$, where a is the separation DE. When O is the zero order fringe of the light from B, then BF exceeds BC by one wavelength. This is the condition for the disappearance of the fringe effect, therefore

$$\theta = \frac{\text{PF}}{\text{CF}} = \frac{\lambda}{b}, \text{ while } \alpha \text{ remains} = \frac{\lambda}{a}.$$

Thus the interferometer in effect magnifies the angular diameter of the star in the ratio $\frac{b}{a}$.

This arrangement, which is probably the most important astronomical development of this century, has a twofold advantage. In the first place, it has a resolving power only limited by the purely physical limitations of the length of girder that can be constructed without undue flexure and vibration. Secondly, even when atmospheric conditions are such that star images with large aperture telescopes are badly defined and present a 'boiling' appearance, the interference fringes may be quite distinct. This is because the apertures in the interferometer are small. Any variation in the index of refraction of the air over one aperture merely causes the fringe system to move as a whole. Provided this motion is not too rapid the distinctness of the bands remains unaltered, while under the same conditions the star image from a full aperture telescope would be considerably impaired.

The first observations were made with a 20-foot interferometer mounted on the 100-inch Hooker reflector at Mount Wilson. This large telescope was selected merely for its mechanical strength and not because of any optical requirements. The inner mirrors $M_2 M_3$ had a constant separation of about 45 inches, giving a fixed fringe spacing of about ·02 mm., easily visible with a magnification of 1600. M_1 and M_4 are symmetrically adjusted so that the two pencils overlap in the focal plane of the telescope. In general, interference bands cross the star image, which is elongated because of the restricted aperture.

Michelson and Pease[15] found that the fringes from the red star Betelgeuse (α Orionis) disappeared when the outer mirrors had a separation of 121 inches, although they reappeared when the telescope was turned on another star, which showed that the instrument was in adjustment. Assuming an effective wavelength $\lambda = 5750$ Å the formula $\alpha = 1{\cdot}22 \frac{\lambda}{b}$ gives the angular diameter of this star to be ·047 seconds.

If the actual star disc (not the diffraction disc as seen

with a telescope) does not radiate uniformly the factor 1·22 is no longer valid. Assuming an intensity distribution $I_x = I_c\,(R^2 - x^2)^n$, I_x being the intensity at a distance x from the centre of a star of radius R, the index n being a measure of the darkening towards the limb, when $n = 0$ the coefficient is 1·22, but for $n = \cdot 5$ (approximate value for the sun) its value is increased by about 17 per cent.

It can be shown that if b_1 and b_2 are the first and second mirror separations at which the fringes vanish

$$n = \frac{5{\cdot}5b_1 - 3b_2}{b_2 - b_1}.$$ *

A 50-foot interferometer is now under construction. With this it will be possible not only to obtain the angular diameters of still smaller magnitudes, but also by estimating the visibility of the fringes at various separations, to deduce the actual intensity distribution over the star disc, which paradoxically we shall never see.

[The light from each point of a star disc contributes equally to form every part of the diffraction disc image through a telescope objective. In this sense the pattern we obtain is not a true image of the star.]

Angular Diameter of Ultra Microscopic Particles

Although Gehrcke [16] suggested it in 1906, the double slit method was not used to measure the diameters of microscopic particles until the principle had been again brought into prominence by the success of Michelson's experiment.

Let AB (Fig. 2.11) represent a short *line* source in front of the microscope objective with C and D as slits. The central bright fringe (zero order) due to A is at F and the next fringe (due to A) is at G. So that $CG - DG = \lambda$. By analogy with the stellar experiment it follows that when the zero order fringe of B coincides with the first order fringe of A the resultant fringes disappear.

* See reference 15.

The fringes vanish when BD − BC = λ. Dropping perpendiculars from A and B on BD and AC respectively (see inset):

BD − BC = (BD − AD) − (BC − AC) = BN + AM (taking A to be symmetrical with respect to the slits so that AC = AD).

If the refractive index of the medium surrounding AB is μ, the optical path difference is μ(BN + AM) = 2μ AB sin $u = \lambda$;

$$\text{or AB} = \frac{\lambda}{2\mu \sin u} = \frac{\lambda}{2\ (\text{Numerical Aperture})}.$$

This Numerical Aperture is not necessarily the full value for the microscope objective, but its actual value

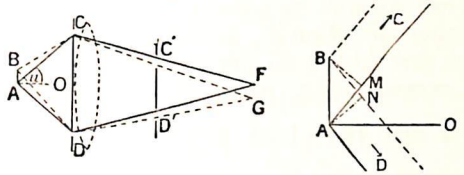

FIG. 2.11.—Gerhardt's Microscope Interferometer

as determined from the positions of the slits. Presumably these can be placed at some other more convenient position C'D' so that they only transmit the same beams as if they were actually at CD.

The double slit method in microscopy has been used by Gerhardt[17] to measure the mercury and mastic particles illuminated in the dark field of a Zeiss cardioid or paraboloid condenser.*

DIVISION OF WAVEFRONT INTO MORE THAN TWO PARTS

The most important example of this class is the Diffraction Grating, and this will be briefly considered so as to afford comparison with the Interferometer methods discussed in Chapter VI.

Suppose for simplicity that we have a plane wavefront of wavelength λ incident normally on a grating of

* In Gerhardt's experiments the particle was only illuminated at its edges, therefore a factor 4 instead of 2 in the above formula has to be applied.

spacing s, the reflecting or transmitting (as the case may be) grooves of which have a width b. If a is the amplitude of the light from a single groove along the normal to the grating, the amplitude in a direction making an angle θ with the normal is

$$a_\theta = a \frac{\sin\left(\frac{\pi b \sin\theta}{\lambda}\right)}{\frac{\pi b \sin\theta}{\lambda}} = a \frac{\sin \mathrm{X}}{\mathrm{X}} \text{ where } \mathrm{X} = \frac{\pi}{\lambda} b \sin\theta.$$

When $\theta = 0$ all the beams arrive at the focal plane of the observing telescope in phase and the resultant amplitude will be $a\mathrm{N}$ where N is the total number of slits. When we wish to obtain the resultant amplitude in any other direction θ, it will be realized that the waves do not arrive in phase. The path difference between corresponding parts of successive beams will be $s \sin\theta$ and the phase difference $\delta = \frac{2\pi}{\lambda}(s \sin\theta)$. We then have to sum:

$$a_\theta \sin wt + a_\theta \sin (wt + \delta) + a_\theta \sin (wt + 2\delta) \ldots + a_\theta \sin (wt + \mathrm{N} - \mathrm{I})\delta.$$

This can be summed trigonometrically, but if it is realized that we are dealing with vector quantities, a simple geometrical method is available.

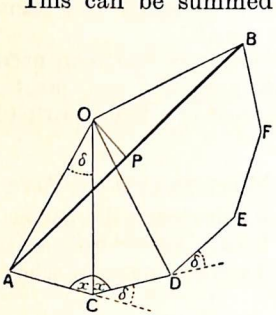

FIG. 2.12.

If the lengths and directions of the successive lines AC, CD, DE, etc., in Fig. 2.12, represent the terms of the above expression in amplitude and phase, then AB will represent the resultant amplitude. In our case AC = CD = DE, etc. Joining the centre O of the circumscribing circle to the points A, B, C, D, etc., and dropping a perpendicular

from O on AB at P, if r is the radius of this circle, we have

$$\angle x = \angle ACO = \angle OCD \text{ and } 2x = 180° - \delta.$$

So that $$\angle AOC = \delta.$$

$$\angle AOP = \frac{N\delta}{2} \text{ and } AB = 2r \sin \frac{N\delta}{2}.$$

In the Δ AOC, $$\frac{\sin \delta}{AC} = \frac{\sin x}{r} = \frac{\cos \delta/2}{r}.$$

$$\text{Resultant} = 2AC \frac{\cos \delta/2}{\sin \delta} \sin \frac{N\delta}{2}$$

$$= \frac{2\, a_\theta \cos \delta/2}{2 \sin \delta/2 \cos \delta/2} \sin \frac{N\delta}{2} = a_\theta \frac{\sin \frac{N\delta^*}{2}}{\sin \delta/2}.$$

Thus the full expression for the Resultant Amplitude is:

$$A_\theta = A. \frac{\sin X}{X} \cdot \frac{\sin NY}{\sin Y}$$

where $Y = \delta/2$ is half the phase difference between the waves from corresponding points of consecutive slits.

The last term varies much more rapidly with δ (or with θ) than the second, so that the sharp line pattern of the diffraction grating is entirely due to the interference effects of the beams from the various grooves; $\frac{\sin NY}{\sin Y}$ has its maximum value N when $Y = 0$ or any integer multiple of π. The minimum values are given by $Y = \frac{K}{N} \pi$ when K is an integer not exactly divisible

* In the special instances where δ can be made infinitely small (with corresponding increase of N) we have :

$$\text{Resultant} = a_\theta \frac{\sin N\delta/2}{\sin \delta/2} = a_\theta \frac{\sin \frac{N\delta}{2}}{\delta/2} = a_\theta N. \frac{\sin \frac{N\delta}{2}}{\frac{N\delta}{2}} = A \frac{\sin \alpha}{\alpha}$$

where α is now $\frac{1}{2}$ the extreme phase difference.

by N, and the first minimum values on either side of a principal maximum $Y = m\pi$, are $Y_1 = \left(m + \frac{1}{N}\right)\pi$ and $Y_2 = \left(m - \frac{1}{N}\right)\pi$.

For a principal maximum $Y = m\pi = \frac{\pi}{\lambda} s \sin\theta$

or that $$s \sin\theta = m\lambda.$$

Hence $\frac{d\theta}{d\lambda} = \frac{m}{s\cos\theta}$ is the dispersion of the grating.

If θ_1 and θ_2 are the directions of the first minima on either side of the principal maximum θ,

$$\frac{\pi}{\lambda} s \sin\theta_1 = \left(m + \frac{1}{N}\right)\pi, \quad \frac{\pi}{\lambda} s \sin\theta_2 = \left(m - \frac{1}{N}\right)\pi$$

$$\text{giving } \frac{s}{\lambda}\{\sin\theta_1 - \sin\theta_2\} = \frac{2}{N}$$

$$\text{or} \qquad \sin\left(\frac{\theta_1 - \theta_2}{2}\right) = \frac{\lambda}{Ns\cos\frac{\theta_1 + \theta_2}{2}}.$$

In an ordinary grating Ns is very large compared with λ, so that $\sin\frac{\theta_1 - \theta_2}{2} = \delta\theta$ the angle between the centre of a maximum and its first minimum and

$$\cos\frac{\theta_1 + \theta_2}{2} = \cos\theta.$$

The late Lord Rayleigh has shown that it is possible to 'resolve' two spectral lines when the principal maximum of one corresponds to the first minimum of the other. Therefore if we make the $\delta\theta$ in the expression for the dispersion equal to $\delta\theta = \frac{\lambda}{Ns\cos\theta}$, the corresponding $\delta\lambda$ will be the smallest wavelength change observable.

This gives $$\delta\lambda = \frac{\lambda^2}{Nm}.$$

The ratio $\left(\frac{\lambda}{\delta\lambda}\right)$ is termed the *Resolving Power* and equals Nm. The order of interference m means, that the path difference between the beams to and from successive grooves is m wavelengths. This leads to another and probably more convenient way of regarding the Resolving Power of a grating. *It is the path difference between the beams incident at the ends of the grating measured in wavelengths.*

As an example, consider the case of a reflection grating, the ruled portion of which is l cms. If it is used in a 'Littrow' or back reflecting method so that the incident and diffracted beams are practically superposed, the Resolving power:

$$\text{R.P.} = \frac{2\ l\ \cos\ \theta}{\lambda}$$

where θ is the angle the light makes with the grating surface. Thus a grating has its maximum resolving power when the incident and diffracted beams are superposed and practically grazing the grating surface.

Echelon Gratings

The R.P. of a grating cannot be increased indefinitely by increasing the number of rulings, since after a certain stage, the diamond point of the ruling machine becomes worn. A large grating with a large spacing of wide grooves cannot be made with sufficient accuracy. This led Michelson[18] to devise an entirely new way of obtaining high resolving power. His method was to pass a parallel beam of light from a collimator through a pile of plates arranged in echelon formation. The beams emerging from consecutive apertures are uniformly retarded and we get a transmission grating of a comparatively small number of apertures, but a very high order of interference $\frac{(\mu - 1)\ t}{\lambda}$, where t is the thickness of each plate and μ its refractive index for the wavelength λ. Full details of the transmission

instrument are given in standard textbooks such as Wood's *Optics* or Preston-Porter's *Theory of Light*.

Recently a method[19] has been found of making Michelson's original idea of using it as a reflection instrument a practical possibility. This has the advantage that its use is not limited by the transmissivity of glass, and it also has between three and four times the resolving power of the corresponding transmission instrument.

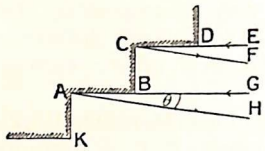

FIG. 2.13.—Path difference in a reflection Echelon

This will now be briefly considered. The path difference GAH — ECF (Fig. 2.13) for light incident normally on the plates CB and AK (AB = CD = t, AK = BC = s) when the light is diffracted at a small angle θ is [20] $\mu_{air}(2t - s\theta)$ and for reinforcement

$$\mu_{air}(2t - s\theta) = m\lambda.$$

Neglecting the dispersion of the air, the dispersion of the grating is:

$$\frac{d\theta}{d\lambda} = \frac{m}{s} = \frac{2t}{\lambda s}.$$

Putting m successively $= m$ and $m + 1$ corresponding to θ_1 and θ_2 directions (and writing $\mu_{air} \simeq 1$), the angle between successive orders $\theta_1 - \theta_2 = \frac{\lambda}{s}$.

As in an ordinary grating, the resolving power is Nm, and while N may only be 25 — 35, the order 'm' for a plate thickness of 7 mm. is 34,000 (λ 4000 Å).

If the light diffracted from each slit had been spread over a wide angle we should have several hundred orders of spectra, but owing to the large width s of each step, practically the whole of the diffracted light is contained in a narrow angle. The expression $\frac{\sin X}{X}$ $\left(X = \frac{\pi s \sin \theta}{\lambda}\right)$ by which $\frac{\sin NY}{\sin Y}$ must be multiplied

has a maximum value when $\theta = 0$, and zero values when $\theta = \pm \frac{\lambda}{s}$, or multiples of this. If $2\mu t = m\lambda$, the principal maximum of $\frac{\sin N\mathrm{Y}}{\sin \mathrm{Y}}$ occurs when $\theta = 0$ and the next orders occur at $\theta = \pm \frac{\lambda}{s}$. Here the factor $\frac{\sin \mathrm{X}}{\mathrm{X}} = 0$, so that no spectra appear. This condition is known as the *Single Order* position of a spectral line. In general we see two orders of line, an angle $\delta\theta = \frac{\lambda}{s}$ apart, which may lie anywhere in the region between $\theta_1 = -\frac{\lambda}{s}$ and $\theta_2 = +\frac{\lambda}{s}$.

In a transmission instrument the variation of path difference needed to change the position from single to double order can be obtained by slightly tilting the Echelon, and this is done without any material displacement or deviation of the spectra.

The same method cannot be used with the Reflection type as the necessary tilting would cause the reflected beam to go outside the field of view.

Fig. 2.14 shows the method finally adopted for

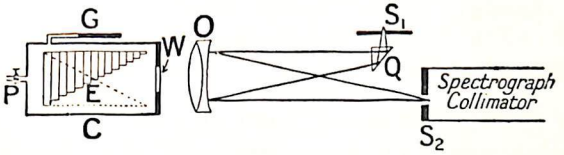

FIG. 2.14.—Combination of a Reflection Echelon and a Spectrograph

using a Reflection Echelon in conjunction with a spectrograph. The light to be analysed is focussed on a primary slit S_1 which may either be vertical or horizontal. It is reflected by the small quartz prism

Q to the objective O and through the quartz or fluorite window W on the Echelon. The reflected beam is focussed by O on to the slit S_2 of the spectrograph. The latter makes a coarse analysis of the spectrum and separates the lines of widely different wavelengths so that these do not overlap as they do at the slit S_2. When S_1 is vertical the edges of the Echelon plates must also be vertical as in the figure, while the slit S_2 must be sufficiently wide to accommodate at least two orders of any line. By also taking a plate with the Echelon turned through two right angles, it is possible to determine whether a satellite lies on the long or short wavelength side of a main line. In the one position of the Echelon, its dispersion assists that of the spectrograph, while in the other, it opposes it. With a very rich spectrum such as that of the iron arc, the slit S_1 and the Echelon plate edges are arranged horizontally so that its dispersion is along the slit S_2 which can now be narrowed down as desired. In order to change a line from single to double order position as required, the air pressure in the chamber C is varied by connecting it to a suitable pump, and provided there is no leakage of air to or from the chamber during an exposure, the pattern remains steady in spite of variations of temperature. This is because the density and consequently the refractive index of the gas in the chamber remains constant, while the expansion of the silica Echelon plates with ordinary temperature changes is negligibly small.

GENERAL REFERENCES

CHEMICAL AND BIOCHEMICAL APPLICATIONS OF INTERFEROMETRIC METHODS

F. Löwe : *Optiche Messungen des Chemikers und des Mediziners* (1925) (T. Steinkopff, Dresden).

APPLICATIONS OF INTERFERENCE METHODS TO ASTRONOMY

A. A. Michelson : *Studies in Optics*, Chapter XI (1927) (Univ. Chicago Press).

A. A. Michelson : *Light Waves and their Uses*, Lect. VIII (1907) (Univ. Chicago Press).

TEXT REFERENCES

[1] Rayleigh : *Proc. Roy. Soc.*, **59**, 201 (1896).
[2] Edwards : *Bull. Bur. Stand.*, **14**, 474 (1917) ; *J. Amer. Chem. Soc.*, **39**, 2382 (1917).
[3] Adams : *Journ. Amer. Chem. Soc.*, **37**, 1181 (1915).
[4] Haber and Löwe : *Zeitschr. f. angew. Chem.*, **23**, 1393 (1910).
[5] Edwards : *Techn. Papers Bur. Stand.*, No. 113 (1918).
[6] Mohr : *Zeitschr. f. angew. Chem.*, **25**, 1313 (1912).
Hilliger : *Zeits. Dampfk. u. Maschinen betr.*, **34**, 165, 200 (1911).
Klemperer : *Chem. Zeitung* (1911), 557.
[7] F. Löwe : *Ann. der Hydrogr.*, **40**, 303, 1912.
[8] Hirsch and Hecker : *Zeitschr. f. angew. Chem.*, **33**, 269 (1920).
Hirsch and Hecker : *Chem. Zeitung* (1920), 691.
Hirsch : *Wochenschr.*, **4**, Nos. 28/29 (1925).
[9] C. F. Löwe : *Chem. Zeitung* (1921), 405.
[10] Michelson : *Phil. Mag.* (5), **30**, 1 (1890) ; *Nature*, **45**, 160 (1892).
[11] Fizeau : *Comp. Rend.*, **66**, 934 (1868).
[12] Stefan : *Comp. Rend.*, **78**, 1008 (1874).
[13] Hamy : *Bull. Astr.*, **16**, 257 (1899).
[14] Michelson : *Astro. Journ.*, **51**, 257 (1920).
[15] Michelson and Pease : *Astro. Journ.*, **53**, 249 (1921).
[16] Gehrcke : *Anwendung der Interferenzen* (1906), p. 120.
[17] Gerhardt : *Zeitschr. f. Physik*, **35**, 697, 1926 ; **44**, 397, 1927.
[18] Michelson : *Astro. Journal*, **6**, 36, 1898.
[19] Williams : Brit. Pat., **312534**.
[20] Williams : *Proc. Opt. Conv.*, II, 987, 1926.

CHAPTER III

INTERFEROMETER ARRANGEMENTS INVOLVING A DIVISION OF AMPLITUDE

WE have seen that, in order to obtain interference phenomena with different *parts* of the same wavefront, the wavefront must be such that its properties in its different parts are similar, to a degree dependent on the fineness or closeness of the fringes. In the Young double-slit experiment or its variants, the Rayleigh or the Michelson star interferometer, if the two secondary slits are very close (producing widely spaced bands) the primary source can be relatively wide.

Another method of obtaining the necessary two or more beams for interference is to divide the whole beam by partial reflection. After division by this method the wavefronts of each part are similar, any peculiarity in the original incident wavefront being shared equally by the two or more resulting beams. A simple illustration of this method is given in the colour effects of thin films—the interference colour effects of soap bubbles or of oil films on a wet road.

When the film is thin, the light can both be complex (in wave-length) and incident on the film at all angles, while the recording instrument may have a fairly wide aperture.

Let t (Fig. 3.1) be the thickness of a parallel plate of refractive index μ. If AB represents the normal to any wavefront S_1 incident on the plate, S_2 and S_3 are the wavefronts reflected from the upper and lower surfaces respectively. The path difference, or the retarda-

tion of S_3 compared with S_2, is $2\mu t \cos\theta - \frac{1}{2}\lambda$ [the phase change effect due to reflection at a denser medium]. When t is small, the *lateral* displacement of the S_3 wavefront from S_2 is small, $GF = 2t \tan\theta \cos i$, and from any one small region BF of the plate, only the light which falls on it at an angle i can be reflected at the same angle into the eye or camera. If 't' varies along the plate then the total retardation between S_2 and S_3 from different points will vary. Since the intensity of the light with two interfering beams is $4a^2 \cos^2 \frac{\Delta}{2}$, where $\Delta = \frac{2\pi}{\lambda}\left(2\mu t \cos\theta - \frac{\lambda}{2}\right)$ a being the amplitude of each beam, the intensity of the light from different points will vary, and the interference effects seem to be situated in the film. With a thin parallel film, the possible variation in θ (or i) may not be sufficient to produce an appreciable change in $2\mu t \cos\theta$, so that the film will appear of practically uniform intensity throughout.

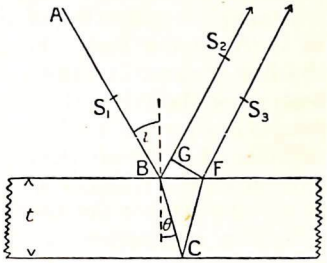

FIG. 3.1.—Interference of thin films

As 't' increases, the localized fringes tend to disappear, but by using a small aperture in front of the eye the condition of one incidence angle to one point of the plate, can be adhered to more closely. This device, e.g. a card with a small hole a fraction of a millimetre, also makes it easier to observe the fringes due to the variation of θ that can be seen in a parallel plate when t has a sufficiently high value.

These bands, when viewed by transmission instead of reflection, are usually known as Haidinger's[1] fringes. He observed them in mica plates and termed them 'lamellar' fringes as distinct from the 'contact' rings

of Newton. They have been studied by Mascart,[2] Michelson [3] and Lummer.[4]

With a parallel plate, a given fringe corresponds to a constant value of cos θ or θ, hence the name of fringes of *constant inclination* given to them by Lummer, and as a given fringe is made up of all rays that have a given fixed inclination to the plate, these parallel rays can be focussed at the focal plane of a telescope objective; in other words, the rings are at infinity, and can be seen with the naked eye without the screen, if the eye is focussed on a distant object, and not on the near-by plate.

The fringes caused by variations of t in a *thin* plate, we have seen originate at these variations; these Lummer termed '*localized*' fringes, corresponding to Haidinger's 'contact rings'.

A simple application of the localized fringes is given us in Newton's Rings, so called because Newton was the first to examine them in detail, although they had been described by Hook in his *Micrographia*. The fringes are formed by bringing in contact two spherical surfaces of different curvatures, or a spherical and a flat surface. When the difference in curvatures is small, the fringes are easily seen with the naked eye, otherwise a low-powered microscope focussed on the point of contact is essential.

With *clean* surfaces, ensuring true contact, the centre spot as seen by *reflected* light is black, showing (as here there is no path difference between the beams reflected at the two surfaces) there must be a change of phase of π at reflection in one or other surface. [Lloyd's single mirror experiment shows this change of phase to occur when light is reflected at a *denser* medium.] The fact that the squares of the radii of successive dark rings are proportional to the natural numbers, depends on the geometry of the circle. It is important to realize that the fringes are so close to the pole of contact, that the reflecting surfaces are sensibly parallel in this region. If x is the perpendicular distance from a tangent to a point on a circle of radius R, then if ϱ is

half the length of a chord drawn parallel to the tangent, $x\ (2R - x) = \rho^2$. So if x is very small compared with 2R, $x = \rho^2/2R$. The path difference between the rays for practically normal incidence is $2\mu x$, where μ is the refractive index of the interspace; thus in consequence of the change of phase, when $\mu\rho^2/R = m\lambda$, we get darkness. This holds for successive integer values of m, so that $\rho_1^2 : \rho_2^2 : \rho_3^2 : : 1 : 2 : 3$, ρ_1, ρ_2 being the radii of the successive *dark* rings, the centre dark spot corresponding to $m = 0$.

The rings may be regarded as contour maps, one fringe for each half wavelength [since the light for interference has to travel the double journey], hence if we look at the fringes in an inclined direction they become elliptical. As it is difficult to get much light to enter the lens under this condition, it is better to put the lens surface under one side of a prism. If the interface is illuminated from a second surface, the elliptical rings can be clearly seen through the third face.

If in any of these arrangements, the plane and sphere are gradually separated, the fringes close in, until when the separation is a quarter of a wavelength, the bright and dark rings have interchanged position. We have thus a very sensitive displacement measurer which has been applied to a variety of uses. Thermal expansion and magneto-striction, for example, can be measured by this means.

With a concave lens of air, as we have in Newton's rings, the rapid closing up of fringes away from the centre is unfavourable for accurate measurement. It is better to use a wedge film, when the bands will be uniformly separated. When the wedge is an air wedge, the number of bands per unit length is twice the angle (in radians) divided by the wavelength measured in the same unit.

If AB and AC (Fig. 3.2) are the two surfaces of the wedge, at A the path difference is zero, at B or C the path difference between the rays is 2BC.

Then $2BC = n\lambda$, if B coincides with the nth dark fringe counting from A. Thus since $BC = al$ where $l = AB$, $n = \frac{2\alpha}{l\lambda}$; when the wedge has an index μ, the optical path difference becomes 2μ BC, and for the same wedge angle the number of fringes per unit length increase to μ times its former value. Taking an average value of 5000 Å for the wavelength, 1 fringe per cm. in an air wedge means an angle of 5 seconds, while if it be a glass wedge it corresponds to an angle of $3\frac{1}{3}$ seconds ($\mu = 1{\cdot}5$).

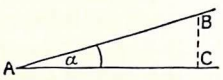

FIG. 3.2.—Wedge angle by interference method

Fizeau [5] used this method for studying the thermal expansion of crystals. The unit of measurement is so small that only a short length of crystal and a small rise of temperature are required to give measurable results. A plate of quartz 5 mm. thick will give a displacement of 9 complete fringes on being heated from 10° C. to 50° C. Tutton [6] has devised an improved form of Fizeau's apparatus. The main difficulty is to prevent any alteration in the position of the reference plane due to temperature. If the crystal rests on a base plate and the reference plate on points of metal pillars attached to the base, the pillars will expand on rise of temperature and the fringe shift observed will be due to the *differential* expansion of the crystal and the metal, the expansion coefficient of which must be determined independently. A correction was made for the variation of the refractive index of the air film with temperature.

It will be readily seen that these interference bands from their films or wedges can be used in a variety of ways to measure, for example, the elastic constants of materials. The extensions and deformations required for accurate measurement are so small, that there is no approach to the elastic limit. An ingenious example is the determination of Poisson's ratio by bending a

flat lath of the material; it is shown in textbooks on the Properties of Matter that the Poisson constant is given by the ratio of the curvatures along, and perpendicular to, the length of the lath.

If AOB (Fig. 3.3) represents the working surface of a lens and LM the circular section of the bent blade, let R be the radius of curvature of AOB, ϱ_1 that of LOM in the plane of paper, and ϱ_2 in the plane perpendicular to it. The path difference between a ray that is reflected approximately normally from C and E = 2(CD + DE).

$$CD = (FC)^2/2R. \quad DE = (FC)^2/2\varrho_1.$$

Let r_1 be the radius FC of a ring in the plane of the

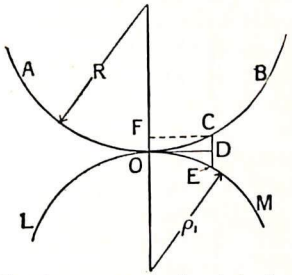

FIG. 3.3.—Elastic constants by interference fringes

paper and r_2 its radius perpendicular to this. In the plane of the paper, the path difference $= r_1^2\left\{\frac{1}{R} - \frac{1}{\varrho_1}\right\}$; for the *same* ring in the other plane the path difference $r_2^2\left\{\frac{1}{R} - \frac{1}{\varrho_2}\right\}$ must be the same.

$$\text{Thus } \frac{r_1^2}{r_2^2} = \frac{\left(\frac{1}{R} - \frac{1}{\varrho_2}\right)}{\left(\frac{1}{R} - \frac{1}{\varrho_1}\right)} = \frac{\left(1 - \frac{R}{\varrho_2}\right)}{\left(1 - \frac{R}{\varrho_1}\right)}.$$

Knowing R. and various corresponding values of r_1 and r_2, the value of Poisson's Ratio ϱ_1/ϱ_2, can be calcu-

lated for each fringe. The innermost fringes cannot be very accurately measured since the fringes themselves are relatively broad. A very large radius of curvature R can only be used with an optically polished lath with very small loads, since when the deformation curvature in one azimuth becomes identical with R, the elliptical fringes become straight lines.

These fringes are widely used in precision engineering for comparing gauges, which are usually in the form of rectangular cubes. The standard G and the comparison T gauges (Fig. 3.4) are wrung in contact with a plate of known flatness. [In this process both the plate and the under side of the gauges are carefully cleaned and freed from motes. With the help of a little clean paraffin and pressure, the surfaces can be made to adhere.] The gauges are placed some definite distance L apart. The top surfaces are cleaned and another clean optically flat plate is allowed to rest on top. Fringes will in general be seen between the tops of the gauges and the lower surface of the upper plate. If the upper surface of T is parallel with that of G, the number of fringes per unit length over each will be the same. If l is the width of the standard gauge which shows n fringes (the fraction, if any, can be estimated) the angle δ that the plate makes with its surface is $\left(\frac{n\lambda}{2l}\right)$, so that if L is the separation between G and T as shown, the block T is $\frac{n\lambda L}{2l}$ longer than the standard G.

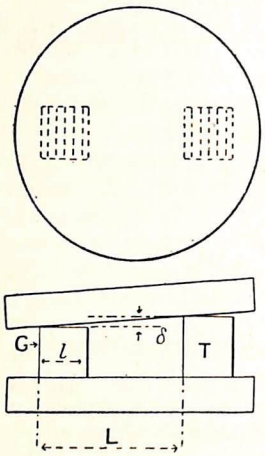

FIG. 3.4.—Gauge testing by interference method

In using this arrangement, care must be taken that

the measurement L is made between the bearing points. If the upper surface of T is not flat but inclines towards G, the value of L that must be chosen will be the outside separation of G and T. Whether the difference between the two is a positive or negative one can be quickly determined by gently pressing the centre of the upper test plate. If the bands spread out, then the bearing points of both blocks are on the outside and T is greater than G and vice versa.

In the apparatus that is made by Hilger,[7] a third standard optically flat plate is provided, to be used periodically in checking the flatness of the working plates that may be accidentally deformed or unevenly worn through usage. The bands are observed with white light through a special screen that gives an effective wavelength ·000,02 inches, so that each fringe means a displacement of ·000,01 inches. The optical flats are $2\frac{1}{2}$ inches in diameter; if the bearing edges of G and T are 2 inches apart, and we have 40 fringes per inch, which is not too fine for counting, the difference in size is $40 \times 2 \times \cdot000,01 = \cdot000,8$ inches. Thus the method follows very conveniently on the limit of a micrometer screw measurement.

As an illustration of the accuracy obtainable with this method in testing the flatness of a surface, Rayleigh,[8] who tested the flatness of a test plate by immersing it on levelling screws just under the surface of water in a trough, points out that a margin of about $1\frac{1}{2}$ inches is desirable to avoid the curvature effect due to capillarity at the edges.

Before leaving the interference effects of thin films, two important properties must be mentioned. In the first place, the patterns observed by reflected and transmitted light are always complementary, the maxima of one system corresponding to the minima of the other. This was verified by Arago,[9] who showed that the fringes in a Newton's Ring experiment vanished when light sources of equal brightness were placed in front and behind the apparatus. Indeed Lummer [10] has

devised an Interferential Photometer based on this principle, the vanishing of the reflected and transmitted fringes indicates an equality of intensity of illumination at the thin film, which in this case is an air film formed between the hypotenuse faces of two 90° prisms. The sensitiveness is of course not high.

At the beginning of the chapter, it was assumed for simplicity that we were only concerned with interference effects between two wave trains of *equal* amplitude reflected at each surface in the film. This cannot be strictly so, for if the first surface reflects a fraction f, the second surface has a lower amplitude incident on it, so that its reflected wave will have a still lower value. Actually, we have multiple reflection occurring in the film and wavefronts of decreasing amplitude are transmitted and reflected. This was pointed out by Poisson ; [11] the practical effect is an appreciable sharpening of the fringes. The actual distribution is discussed later in connection with the Fabry Perot Interferometer. It is shown most clearly in Herschel's [12] fringes obtained by placing a prism on a flat glass or metal plate. In the neighbourhood of the critical angle, the reflecting power of the hypotenuse face is high, thus aiding multiple reflection and the fringes are sharp, while as the angle of incidence becomes more normal, the bands become more diffuse.

It is interesting to notice that with Herschel fringes, a comparatively large separation of the surfaces only gives a low order of interference, since the angle r of the ray in the film approaches 90°, and the path difference is $2\mu t \cos r$.

Brewster's Fringes and Jamin's Interferometer

Consider light incident on two parallel plates of equal thickness making a small angle α with each other as in Fig. 3.5. Some light will be reflected at each of the four surfaces. Of the remainder, a part will undergo internal reflection at one plate A and be reflected from the outside surface of B (Beam 1 in Fig.) Another part

will undergo the internal reflection in B only. The path difference introduced by a single internal reflection is $2\mu t \cos r$, where r is the angle of refraction (and reflection in the glass). The path difference between 1 and 2

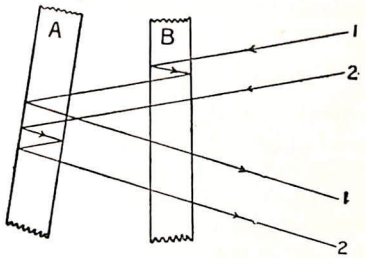

FIG. 3.5.—Arrangement for Brewster's Fringes (Refraction in the Plates omitted (for simplicity).

(the latter has been drawn beneath instead of superposed on 1, merely for clearness) is therefore

$$= 2\mu t \{\cos r_A - \cos r_B\}$$
$$= 4\mu t \sin \frac{(r_B + r_A)}{2} \cdot \sin \frac{(r_B - r_A)}{2}.$$

When the light is incident symmetrically between the normals of the two plates, the angle of incidence on each is $\frac{\alpha}{2}$ and $\angle r_A = \angle r_B$ so that there is no path difference for this incidence. As the angle of incidence increases, $\{\cos r_A - \cos r_B\}$ also increases approximately uniformly so that we get a series of fringes running parallel to the edge of the air prism formed by the plates. Since the path difference for a given set of plates at a fixed angle depends only on the angle of incidence and not the relative position of the beam, the fringes, like Haidinger's rings, are at infinity.

Beams that have undergone two and three internal reflections will have twice and three times the above path difference, and as in the case of thin films, the dark space between the bands is appreciably wider than the bright fringe.

These fringes were first observed by Brewster [13] and suggested to Jamin [14] the basis of a method of constructing an Interferential Refractometer which, until the more accurate Rayleigh instrument became available, has been extensively used in determining small differences of refractive index.

Jamin Interferometer

The instrument essentially consists of two plane parallel slabs of glass of exactly the same thickness. [A pair is usually cut from a single plane parallel piece from 2 to 5 cm. thick.] The plates are silvered on one side and are mounted as shown in Fig. 3.6. The lens L, which is not however essential, is spherocylindrical and merely serves to illuminate the plate P_1 uniformly.

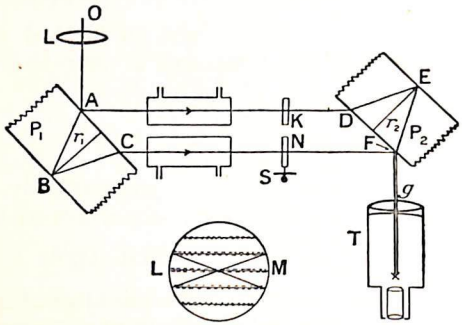

FIG. 3.6.—Jamin Interferometer and Field of View

A beam of light OA divides at A, a part is refracted and then reflected at the silver film B to emerge from C to F. Of the other part AD a fraction enters the second plate P_2, is reflected at E and emerges at F. The two beams travelling along Fg enter the telescope T. The path difference between the two beams is as before:

$$2\mu t \{\cos r_1 - \cos r_2\}$$

which is zero when the plates are parallel. If now one plate is tilted along a horizontal axis parallel to its

surface so that the normals to the plates, while parallel in the horizontal plane, make a small angle α in the vertical plane, a beam from O, making an angle $\frac{\alpha}{2}$ with the horizontal plane, will have the same incidence angles on both plates, so that $r_1 = r_2$. This will be true whatever angle OA makes in the plane of the paper, since in this plane the sections of the surfaces are parallel. Another beam O_1A_1 parallel to the first, but displaced, will emerge parallel (but displaced) to Fg and come to a focus at the cross wires of the telescope. As OA varies in the vertical direction, the path difference introduced alters and we have a series of horizontal bands that are very nearly straight, as shown in the inset. The greater the angle of inclination between the normals, the closer the fringes.

The plates P_1 and P_2 are made thick, so that there should be a liberal separation between the beams AD and CF. If a pair of similar tubes with optically flat end pieces be placed in the path and one of the tubes gradually evacuated, a given fringe LM will move across the field. If 'l' is the length of the chamber and $\Delta\mu$ the change in refractive index,

$l.\ \Delta\mu = n\lambda$, where n is the number of fringes displaced by the change, and λ the wavelength.

To obviate the labour of counting numerous fringes, Jamin devised the compensator that we have already met in the Rayleigh instrument. Here both plates are adjustable according to the sensitiveness required. [At perpendicular incidence, a larger rotation is required to produce a given path difference.] Instead of a lever and screw motion, a circular scale is attached to the moving plate. The Jamin is adjusted in the following way. The plates P_1 and P_2 are first roughly set in position, and the source, say a sodium burner with a small diaphragm in front, is placed about 2 metres behind the instrument. The central images are arranged to overlap and the source brought (without diaphragm)

within about 10 cm. from L. Generally speaking, inclined fringes are seen in the field. The plate P_2 can then be adjusted until these spread out, and the whole field is of uniform colour; P_2 is then tilted on a horizontal axis DF, when horizontal fringes appear. With a white light source the usual white light fringes can be seen in this position, but if the mirrors be parallel in the vertical plane and make a small angle in the horizontal, white light fringes cannot be obtained with the now vertical fringes.

An essential difference between these fringes and those of Brewster is, that the sizes of the plates are so chosen, that only a single internal reflection can occur at each plate, so that we are dealing strictly with two beams which give a $\cos^2\theta$ intensity distribution, the bright and dark bands being equally wide. There is no need to introduce any diaphragms to limit the beams, as the ends of the gas chambers themselves act as efficient stops.

As a sensitive Refractometer, the Jamin is not as accurate as the Rayleigh, since cross wire settings have to be made. A movement of a plate will displace the bands without displacing the fiduciary mark. In addition, since it needs a more or less extended source, it is not very convenient to use for extended measurements from a rich source, e.g. Iron lines.

In order to obtain a still larger separation of the beams, Mach [15] and Zehnder [16] have used four separate plates, the ones corresponding to the inner surfaces of the Jamin plates being half silvered and the others heavily silvered.

Sirks [17] and Pringsheim [18] have developed a form of Jamin's instrument with the plates wedge shaped. As will be seen from the discussion on wedge-shaped Lummer Gehrcke plates (page 101), the fringes are no longer at infinity but are localized at a point dependent on the wedge angle of the plates. They are observed by means of a microscope, hence the name Interference-microscope that has been given to the combination.

Its especial advantage is that with localized fringes, clear fringes can be obtained with very narrow beams, so that the method is suitable for determining index changes of substances that can only be obtained in small quantities.

REFERENCES

[1] Haidinger : *Pogg. Ann.*, **77**, 219 (1849).
[2] Mascart : *Ann. d. Phys. et Chim.* (4), **23**, 116, 126 (1871).
[3] Michelson : *Phil. Mag.* (5), **13**, 236, 1882.
[4] Lummer : *Wied. Ann.*, **23**, 49, 1884.
[5] Fizeau : *Ann. d. Chim. et Phys.*, (4), **2**, 147 (1864) ; **8**, 335, 1866.
[6] Tutton : *Phil. Trans.*, **191**, 313, 1898.
[7] Cf. Smith : *Machinery*, Oct. 27, 1927.
[8] Rayleigh : *Proc. Roy. Inst.*, **14**, 72, 1893 ; *Nature*, **98**, 212, 1893.
[9] Arago : *Œuvres*, vol. 10, p. 16 ; cf. Young : *Misc. Works*, **1**, 381.
[10] Lummer : *Verh. d. Deutsch. phys. Ges.*, **3**, 131 (1901).
[11] Poisson : *Ann. d. Chim. et Phys.*, **22**, 1823.
[12] Herschel : *Phil. Trans.*, **99**, 274, 1809.
[13] Brewster : *Trans. Roy. Soc.*, Edin., **7**, 435, 1817.
[14] Jamin : *Comp. Rend.*, **42**, 482 (1856) ; *Ann. Chim. Phys.* (3), **52**, 163, 1858.
[15] Mach : *Sitzb. d. Wiener Akad.*, **101**, IIA, 5 (1892) ; *Akad. Anseiger*, 1891.
[16] Zehnder : *Zeitschr. Instrumentenkunde*, **11**, 275, 1891.
[17] Sirks : *Handl. Ned. Nat. en Geneesk Congr. Gronigen* (1893), p. 92.
[18] Pringsheim : *Verhandl. d. phys. Ges.*, Berlin, **17**, 152, 1898.

CHAPTER IV

THE MICHELSON INTERFEROMETER AND ITS APPLICATIONS

IN its better-known form, this instrument is an example of division of amplitude considered in the previous chapter. It has however been of such primary importance in both pure and applied Physics, that this chapter will be devoted entirely to it.

The essential idea in the Michelson Interferometer is to divide a beam into two portions at a half silvered plate and to recombine *them at the same plate* instead of effecting the recombination at a second half silvered plate as in the Zehnder and Mach variants of the Jamin Interferometer.

The basic principle was first given in the now famous experiment of Michelson [1] on the relative motion of the Earth and the Aether in 1881. Fig. 4.1 shows a simplified diagram of the interferometer. The light from the source S (which ordinarily is an extended source) is divided at the lower surface of the plate O, which is half silvered, into two beams which fall normally on the mirrors A and B. The returned beams reunite at the same half silvered surface of O and enter the observing telescope T.

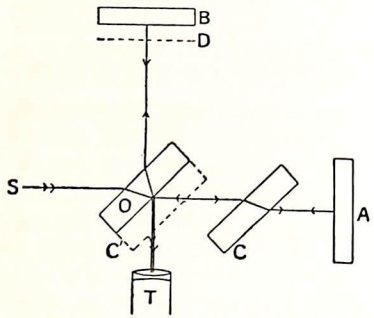

FIG. 4.1.—Michelson Interferometer

Since the light from S that is reflected to B, passes through the plate O three times as compared with the single passage of that going to A, a compensating plate C of the same thickness and material is placed in the OA beam parallel to O. [For convenience the compensating plate is sometimes placed at C′ to save space and to ensure the necessary parallelism of the plates. When the half silver film is on the upper surface of O, the compensator plate C has to be on the OB side.]

Consider the case when the plane mirrors A and B are perpendicular and the dividing mirror O is at 45° to either. If OA is slightly less than OB, the image of A in O is at plane surface D parallel to B. In the telescope then, we shall observe the interference effects of a parallel plate. These will be a series of rings corresponding to directions when $2\mu_{\text{air}}\ t\ \cos\ \theta = m\lambda$, t being the perpendicular distance BD and θ the angle of incidence (and reflection) corresponding to one particular ring and m an integer. As previously explained (page 33), when t, the thickness of the equivalent plate becomes very small, the diameter of the first ring becomes greater than the aperture, so that the whole field is of uniform intensity given by $4A^2\cos^2\frac{\Delta}{2}$, where A is the amplitude of either beam and Δ is the phase difference caused by the difference of path. [It is assumed that the thickness of silver has been chosen for greater efficiency, so that the two beams entering T have the same intensity. Within fairly wide limits of silvering, this will hold, as there is one reflection and one transmission through the silver film for each beam.]

This ring system at infinity, which disappears for very small and zero values of t, has an important distinction from the Haidinger fringes which it superficially resembles. These fringes are true $\cos^2\theta$ fringes, so that the dark and bright rings are of exactly equal width; this follows since we have only *two* interfering beams.

When t is large and the surfaces of B and D are not parallel, all traces of interference fringes vanish. If, however, t is very small, a set of fringes may be seen localized at BD, when the surfaces are not exactly parallel. The exact shapes of these fringes have been investigated by Michelson [2] and Feussner [3] and more recently by Krause.[4] It is sufficient for our purpose to realize that they approximate to straight lines, the fringes becoming clearer as t is decreased, or with a given fairly small value of t, as the diaphragm or aperture (in front of the eye or telescope) is decreased.

White Light Fringes

When the surfaces B and D intersect, localized fringes can be obtained with a white light source, the central bright fringe coinciding with the line of intersection of the plates. The colours of the fringes on either side become impure until they vanish (after 3 or 4 fringes) owing to overlap. For a bright fringe the value of $\frac{2t \cos \theta}{\lambda}$ should be an integer; the inclination θ varies but slowly from one band to the other, so that the effect is due to the increasing 't'. It thus follows that a coloured fringe is violet on the side nearer to the central fringe and red on the side remote.

If a very thin parallel plate of thickness 'd' and refractive index μ be placed in the beam near either A or B and covering half the field of view, the fringes through the plate are displaced. Neglecting the effect of the dispersion of the material of the plate, the retardation produced by it is $2d\ (\mu - 1)$, the air having been replaced by the material. Since a displacement of one complete fringe is equivalent to a retardation of one (mean) wavelength, the thickness for a retardation of x fringes is $d = \frac{x\lambda}{2\ (\mu - 1)}$, the thickness being given in the same unit as that in which the main wavelength λ is measured.

Johonnot [5] using a Michelson Interferometer in this way measured the retardation produced when light is passed through the 'dark spot' of a soap film. He found it necessary to have fifty such films in series to obtain a displacement of half a fringe, showing that the retardation for a single transmission through one film d $(\mu - 1)$ is one two-hundredth part of a wavelength.

Visibility Curves and the Fine Structure of Spectral Lines

Fizeau [6] in 1862 observed that at the 500th order or Ring in a Newton's Ring experiment with a yellow sodium source, the fringes had practically disappeared, while they regained their original clearness when the order increased to 1000. [The high order was obtained by separating the lens and plate.] This means that the source was double, and that the 1000th ring of the longer wavelength then coincided with the 1001th of the shorter, so that the wavelength difference was 1/1000 of either wavelength.

Michelson's [7] first application of the new Interferometer was an extension of this principle, by means of which he made a systematic analysis of the more important spectral lines. Instead of merely observing the path differences at which the fringes vanished, he made visual estimates of the clearness or Visibility of the bands for various path differences. The visibility of a fringe was defined as $V = \frac{J_{max} - J_{min}}{J_{max} + J_{min}}$, where J_{max} is the brightness of the centre of a bright fringe and J_{min} that of the centre of the dark fringe on either side; thus the fringes have greatest clarity when $V = 1$ and disappear as V approaches zero.

The observed Visibility curve is the resultant intensity curve for a number of homogeneous sources of different intensities and frequencies. The Visibility-path difference curve for a truly monochromatic source would be a straight line parallel to the axis and the actual Intensity curve a $\cos^2\theta$. Hence what in effect is needed,

is a method of analysing the observed curve into its Fourier components. As Rayleigh [8] has pointed out, a unique correct result can only be obtained if the original line or group of lines be symmetrical. This analysis Michelson effected by means of his 'Harmonic Analyser', a mechanical device which is described in his book *Light Waves and their Uses*, page 68. As an illustration of the accuracy of the method, Michelson found in 1892 that the Red Balmer (Hydrogen) line was a doublet with a separation of ·14Å; the value given by Houston [9] for the separation of the principal components is ·1358Å. In this way Michelson found that Cadmium Red was a

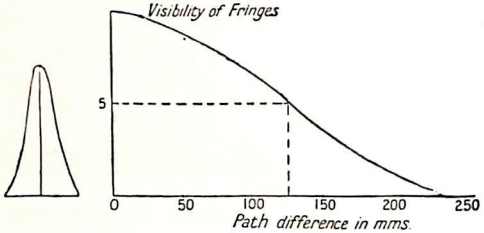

FIG. 4.2.—Visibility curve of Red Cadmium

single line having a half width (i.e. half width at half the intensity of the maximum) of ·0065 Å and a probability curve Intensity distribution. The method has not hitherto been much used outside Michelson's laboratory, partly because of the skill required in its application and partly because the Echelon and Fabry Perot Interferometer show objectively what has to be inferred by the above method. It is however important, not only because it gave us our first knowledge of the fine structure of spectral lines, but that *the resolving power is unlimited.*

We have seen that the circular fringes at infinity must be used with this method, and consequently for large path differences, the rings become very fine, so that it is more difficult to estimate the visibility. If the Twyman and Green modification of this instrument

(see page 65) were used, the localized fringes could be employed ; these can be arranged to any convenient size, and if the ' ways ' or grooves, in which the movable mirror moves, are sufficiently true, the fringes keep the same separation independently of the path difference. Thus photographs could be taken at regular intervals and the visibility measured with high precision by an instrument such as the Moll Microphotometer. The method is not suitable for a complex group as is found in the green mercury, but would be ideal in examining the hyper fine structure of a satellite that could be isolated by means of a powerful auxiliary instrument.

Light Waves as Units of Length

Michelson's [10] next application of his Interferometer was, in collaboration with Benoit, to determine the number of light waves in the standard metre, kept at the International Bureau of Weights and Measures at Sèvres near Paris. As indicated by the experiments described above, the red line of Cadmium was selected as the simplest and most homogeneous light source available. The obvious method of first setting the movable mirror and one fiduciary mark on the metre coplanar, and then moving the mirror until the second mark was coplanar and counting the fringes, would not do. Not only is there a risk of error in counting (this could be avoided by means of a mechanical counter, using say a photo-electric cell) but the fringes would have disappeared with such a large path difference.

To avoid the necessity of making large counts, Michelson constructed a number of Intermediate sub-standards with mirrors separated by 10, 5, 2·5, 1·25 cm., etc., the smallest one being ·39 mm. These consisted of plane glass mirrors M_1 M_2 (Fig. 4.3) silvered on the front and were held in an L shaped bronze holder, by means of bearing pins, and central springs. The parallelism of the mirrors could be effected by means of a screw S, which, acting on the spring C, moved the upper bearing pin of M_2 slightly backwards or forwards.

A carrying arm H enables the Etalon to be moved without the necessity of touching the essential part A, thus avoiding any temperature changes.

The determination of the number of light waves in the metre involves three separate experiments.

(A) The determination of the number of light waves in the smallest etalon.

(B) Comparison of the intermediate substandards.

(C) Comparison of the largest (10 cm.) substandard with the metre.

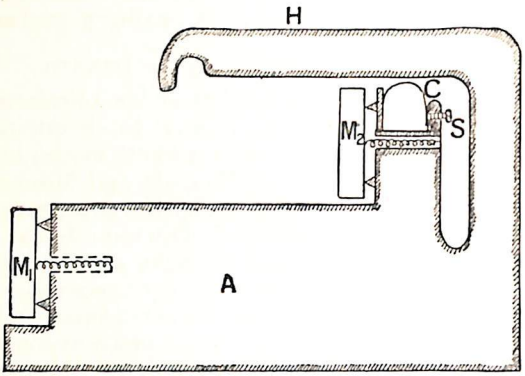

FIG. 4.3.

The form of the interferometer of Fig. 4.1 used in the visibility experiments was slightly modified to that of Fig. 4.4, thus gaining in compactness and greater ease of temperature control. The fixed mirror of the previous arrangement is replaced by one or two of the substandard etalons. The compensating plate C could be rotated about a vertical axis to introduce small path differences when required.

The path differences involved were always small (the largest being with the smallest etalon), so that the localized fringes of thin films could be used throughout, and the telescope T focussed on the small mirrors of

the etalons, the appearance of the field of view being as in Fig. 4.5.

The shortest etalon was evaluated in the following way: AD was made equal to ABM_1, this is obtained when white light fringes are central in M_1. Changing over to red cadmium light which passes from a spectroscope through the slit S (Fig. 4.4) into the interferometer, both M_1 and M_2 are now covered with fringes, since the light is monochromatic. The mirror D is now moved back slowly and the number of fringes crossing any

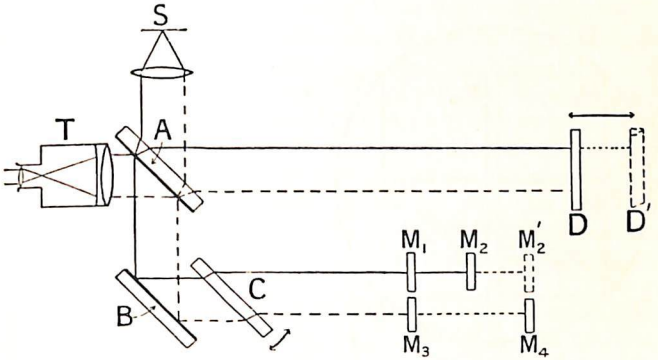

FIG. 4.4.—Michelson's Arrangement for determination of the metre

point on M_2 carefully counted. Since D is to stop at a position D^1, where the white light fringes are central in M_2, the white light source is periodically switched on towards the end of the counting to see that this position is not overreached. The fractional part is determined by tilting the compensator plate C through a small measurable angle, the angle of tilt required for a whole fringe displacement having been previously determined. Though not as homogeneous, the green and blue cadmium radiations were also determined; these served as checks that no whole number errors had been made. The number of red cadmium light waves in the double path of the shortest etalon was

found to be 1212·37 (the fractional part could be determined to within a few hundredths).

The next step of comparing one etalon with the next largest was performed in the following way:

M_1 and M_3 are made coplanar, so that with D in its proper position, white light fringes run continuously across M_1 M_3 as in Fig. 4.5. D is then moved back until the same fringes are central in M_2. The smaller etalon is then displaced until M_1 occupies the previous plane of M_2, which is shown by the reappearance of white light fringes in the lower mirror M_1. D is then moved still further until white light fringes appear in M_2' (the new position of M_2). Red cadmium fringes are then used to count the bands between M_2' and M_4 (assuming M_3 M_4 is slightly greater than twice M_1 M_2), D is moved back still further and the red fringes counted, until, on checking with white light, the achromatic fringes are central in M_4.

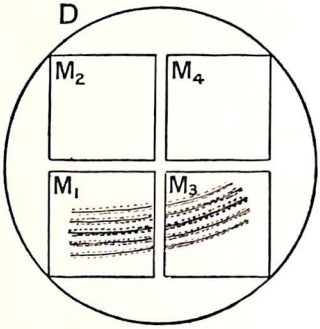

FIG. 4.5.—Appearance of Field of View

It is important to realize that the fractional part of the number of waves in the first etalon is only used to make sure of the whole number value of the red cadmium fringe on proceeding from M'_2 to M_4 so that any error in the first determination is not multiplied up, otherwise the final result would only have the same relative accuracy as the first determination for the smallest etalon. The doubled path of the smaller etalon should contain 2 (1212·37) = 2424·74, so that the next fringe in the measurement of M'_2 M_4 should be 2425, and the final fraction in the second etalon is determined with the compensator C as in the first case.

This procedure is continued until the 10 cm. etalon has been evaluated. The final comparison with the working standard metre is then effected as follows. The fiduciary mark on the standard metre is placed coplanar with the lower mirror of the 10 cm. substandard, by means of a powerful travelling microscope. White light fringes are then obtained by the interferometer in the upper mirror of substandard. The substandard is then moved up until the fringes appear in the lower mirror, which will now be coplanar with the upper mirror in the previous position. The reference mirror is then moved out until the white light fringes are again seen in the upper mirror. This stepping out process is carried out ten times, until the upper mirror is close to the other fiduciary mark on the metre. The *difference* between 10 times the substandard and the metre is then obtained by changing over to red cadmium light and counting the fringes from this last position to that where the mirror and metre mark are coplanar, as shown by a travelling microscope at the other end.

It will be realized that, although the error in the 10 cm. etalon is multiplied in the stepping out process, the total error introduced this way will be much smaller than the errors possible in deciding the alignment of the metre marks and the mirrors. If the working standard metre had been of similar design to the substandard, i.e. two parallel mirrors, instead of somewhat coarse rulings on a straight bar, the probable accuracy would be about ten times greater, for it must be borne in mind that the original prototype metre, which is not handled, has also to be compared with the working standard by means of travelling microscopes. In spite of this, Michelson estimated that his value of 1553163·5 cadmium red waves in the metre at 15° C. and 760 mm. pressure, is correct to about one part in two million.

For other work on the evaluation of the metre, see Chapter VI, page 89.

Velocity of Light in Moving Media

Interferometry has played an all-important part in the advance of our knowledge of this subject, and one experiment, which gave birth to the class of interferometer considered in this chapter, has also led to entirely new conceptions of the relations between the fundamental units of space and time.

Fresnel's [11] calculations of 1818 based on the elastic solid theory of light showed that the ether, or frame of reference for light waves, in a moving medium travelled more slowly than the medium itself, the ratio being $\left(1-\frac{1}{\mu^2}\right)$ where μ is the refractive index of the medium. This was experimentally verified by Fizeau [12] by means of an interferometer somewhat similar to the Rayleigh type described on page 8, with the difference that one of the two interfering light beams always followed, and the other always opposed, the motion of the water in the tubes. With the existence of this Fizeau drift, we can easily explain Airy's observation that the Bradley aberration angle was the same whether the telescope tube be filled with water or air. Fizeau's result was verified by Michelson and Morley and more recently by Harress [13] and Zeeman.[14] The latter's results verified a correction of Fresnel's ratio, first given by Lorentz, for the general case where the moving medium has the property of dispersion.

Babinet and Hoek attempted to find whether there was any *relative* motion between the ether and the earth due to the latter's large velocity through space. Their experiment was repeated by Mascart and Jamin,[15] and the arrangement is shown in Fig. 4.6. Light from the source S, limited by a diaphragm D, is reflected by a half silvered mirror M on to the plate P*l* of a modified Jamin interferometer. The other plate has been replaced by a right-angled prism P*r* so that the optical paths are coincident, with the difference that while the beam (1), reflected at the first surface of P*l*, travels in

a clockwise direction, the other travels in a counter clockwise sense. The two beams meet to produce interference fringes in the telescope T. If the apparatus be adjusted that the line AB is perpendicular to the direction of the earth's motion, the addition of a tube of water W will have no influence on the fringes, since both beams pass through the tube. On rotating the whole through 90°, so that W now lies in the direction of the earth's motion a displacement of the fringes would be expected, for the one beam traverses the water in the direction of the earth's motion, and the other

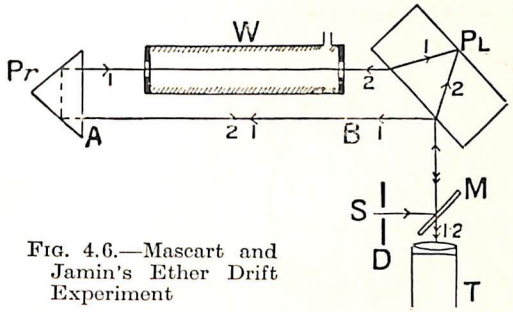

FIG. 4.6.—Mascart and Jamin's Ether Drift Experiment

the opposite. No evidence of such a displacement was found.

The same problem was investigated by Michelson[16] and later, on a larger scale in conjunction with Morley,[17] with a modification of the arrangement in Fig. 4.1.

It is shown in text-books on Relativity and Optics (cf. Preston's *Light*, 5th Edition, page 566) that if D is the distance from the dividing mirror to either of the fixed mirrors of this interferometer, and if one arm of the interferometer is in the direction of the earth's motion, that path will be longer than the other by an amount equal to $\frac{D}{\lambda} \cdot \frac{v^2}{c^2}$ wavelengths, where v is the earth's relative velocity, c the velocity of light, and λ the wavelength. For a rotation of the whole apparatus

through 90° in the horizontal plane, the positions are reversed, so a double displacement of $\frac{2Dv^2}{\lambda c^2}$ is to be expected.

Although it is only a second order effect in terms of $\frac{v}{c}$ which is already small, $\frac{D}{\lambda}$ can be sufficiently great to show its existence even if the effect be less than a twentieth of the expected value. The large path was obtained by reflecting the beams from the dividing mirror M (Fig. 4.7) as shown, keeping the beams approximately parallel to each other. (In the actual experiment four mirrors were used at each corner instead of two as shown in the diagram.) The compensator plate C is placed in the appropriate arm either at C or C_1 according to which side of M is half silvered, as discussed on page 47.

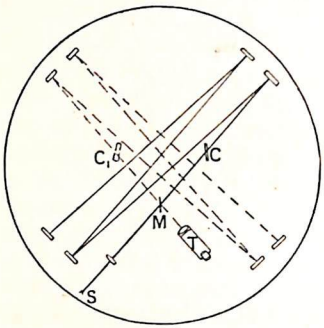

FIG. 4.7.—Michelson and Morley Experiment

The whole was mounted on a rigid base floating on mercury, and arranged to rotate uniformly, readings of the position of the central fringe being taken every sixteenth of a revolution. With a fixed ether, a shift of ·4 of a fringe would be expected; careful observations over an extended period failed to show the existence of a real (as distinct from a temporary effect due to local temperature variations, etc.) displacement of less than a tenth of this amount.

This negative result suggested to FitzGerald and Lorentz that the physical paths actually contracted by an amount just sufficient to compensate for the calculated difference, and with this starting point the theory of Relativity, which has had such a profound influence

on modern physical concepts, was built up—mainly by Lorentz, Minkowski and Einstein.

A repetition of the experiment by Miller [18] seemed to indicate a small but real displacement, but the recent work of Kennedy [19] and Illingworth [20] justifies the conclusion of Michelson and Morley that no observable displacement occurs.

A very interesting refinement has been introduced by Kennedy which will probably find many uses in future Interferometry. One of the mirrors has a thicker film of silver over one half of it than over the other. The

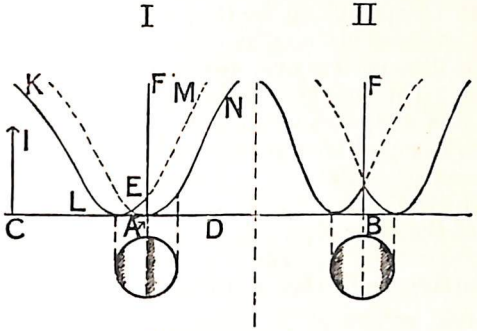

FIG. 4.8.—Kennedy's Half Shadow Method of detecting small displacements

result is to have a raised step of about one-twentieth of a wavelength. The interference fringes instead of running uniformly over the surface of the mirror are discontinuous at this step since the two systems are out of phase by the equivalent of a tenth of a wavelength. If AF in Fig. 4.8 represents the dividing edge on the face of the mirror represented by the base CD, the curve KLEM would represent the $\cos^2\Delta$ intensity curve of a wide fringe parallel to the line AF if the two parts were coplanar. Since the other half is displaced, there is a discontinuity at E and for this half the intensity distribution is AN. The appearance

of the field of view in the immediate neighbourhood of the separating line is shown diagrammatically underneath, the left-hand side is dark and the right-hand side considerably brighter. When the main fringe is displaced so that the minimum is symmetrical about the separating line as shown in II, the line can be made to vanish due to equal brightness on either side. A very small displacement of the main fringe system will cause one part to brighten up and the other half to darken. In the diagram the bands are drawn fairly close together, while in practice, by adjusting the parallelism of the two emerging beams more closely, they can be spread out so that the whole of the field of view is covered by a very small part of a fringe, when the illumination over any one half will be sensibly constant. The method is really equivalent to the half shadow method introduced by Jellet in Polarimetry. Illingworth found that by this method a displacement of between $\frac{1}{1500}$ and $\frac{1}{5000}$ of a fringe could be definitely detected, the exact value depending on the visual acuity of the observer.

Michelson's [21] Earth Rotation Experiment

The null results of all other terrestrial experiments made to test the Relativity theory make this experiment, which should give a positive result, of considerable interest. It was first suggested by Michelson in 1904, but owing to the very high cost was not carried out until 1925.

Consider the paths of the two beams divided at A (Fig. 4.9) and following the square paths ABCDA and ADCBA, in a mean time T_m. If, due to rotation of the earth about the pole, the mirrors are rotating with a linear velocity v the path difference between the clockwise and counter-clockwise beams is

$$D = 4l + v\ T_m - (4l - v\ T_m) = 2v\ T_m.$$

If T_1 is the time for the clockwise beam ADCBA, and T_2 for the other,

$$T_m = \tfrac{1}{2}(T_1 + T_2) = \tfrac{1}{2}\left\{\left(\frac{4l}{c-v} + \frac{4l}{c+v}\right)\right\} = \frac{4cl}{c^2 - v^2}$$

where c is the velocity of light, which being large compared with v gives us

$$T_m = \frac{4l}{c} \text{ with sufficient accuracy, so}$$

that the path difference in wavelengths is

$$\frac{2v.\ T_m}{\lambda} = \frac{8vl}{c\lambda}.$$

If ω be the angular velocity of the earth, we can write approximately $v = \frac{l}{2}\omega$, so that if we write A for the area l^2, the path difference is $\frac{4 \text{ area} \times \omega}{c\lambda}$ wavelengths. If the experiment be carried out at a place of mean latitude θ, the band displacement is $\frac{4 \text{ area} \times \omega \times \sin\theta}{c\lambda}$.

The same result is predicted on the general as well as the special relativity theory. In the general theory it is a test of what is known as the Equivalence hypothesis, and for this reason the experiment was tried.

The mirrors were mounted in boxes at the ends of 12-inch water pipes forming a rectangle 2010 feet by 1113 feet, the pipe at one end was duplicated to accommodate the beam EF in the figure. The whole apparatus was evacuated to a pressure of 12 to 25 mm. of mercury by a 50 h.p. pump. This was necessary to avoid fringe tremor due to temperature irregularities. The system ABFEA served as a fiduciary to give the fringe dis-

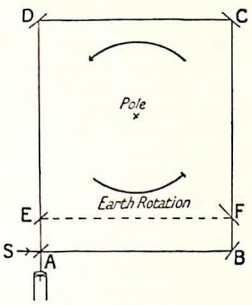

FIG. 4.9.—Michelson's Earth Rotation Experiment

placement due to the effective area EFCD. The mean or effective wavelength of the 20 ampere arc source was found by a subsidiary experiment, and the observed displacement of ·230 ± ·005 fringes agreed well with the calculated value (on both theories) of ·236 ± ·002 fringes.

GENERAL REFERENCES

Michelson : *Light Waves and their Uses.*

TEXT REFERENCES

[1] Michelson : *Amer. Journ. Sci.* (3), **22**, 120, 1881.
[2] Michelson : *Phil. Mag.*, 5 Ser., **13**, 520, 1882.
[3] Feussner : cf. Winkelman's *Hand. d. Phys. Optik.*, 2nd Edit., p. 992, 1906.
[4] Krause : *Ann. d. Phys.* (4), **36**, 383, 1911.
[5] Johonnot : *Phil. Mag.* (5), **47**, 501, 1899.
[6] Fizeau : *Comp. Rend.*, **54**, 1237, 1862.
[7] Michelson : *Phil. Mag.*, 5 Ser., **31**, 338, 1891 ; **34**, 280, 1892.
[8] Rayleigh : *Phil. Mag.* (5), **34**, 407, 1892.
[9] Houston : *Astro. Journ.*, **64**, 81, 1926.
[10] Michelson and Benoit : *Trav. et Mém. Bur. Poids et Mes.*, Vol. 11, 1895.
[11] Fresnel : *Ann. d. Chim. et Phys.* (2), **9**, 56, 286, 1818.
[12] Fizeau : *Comp. Rend.*, **33**, 349, 1851.
[13] Harres : *Die Geschwindigkeit des Lichtes in bewegten Körper*, Diss, Jena, 1912.
[14] Zeeman : *Proc. Amsterdam*, **17**, 445 ; **18**, 398 ; **19**, 125 (1914–1917).
[15] Mascart and Jamin : *Ann. école norm.*, **3**, 336, 1874.
[16] Michelson : *Am. Journ. Sci.* (3), **22**, 120, 1881.
[17] Michelson and Morley : *Phil. Mag.* (5), **24**, 449, 1887.
[18] Miller : *Phys. Rev.*, **19**, 407, 1922.
[19] Kennedy : *Proc. Nat. Acad.*, **12**, 621, 1926.
[20] Illingworth : *Phys. Rev.*, **20**, 692, 1927.
[21] Michelson : *Astro. Journ.*, **61**, 137, 140, 1925.

CHAPTER V

SIMULTANEOUS DIVISION OF AMPLITUDE AND OF WAVEFRONT

WHEN the complex beam from an extended source is divided by means of a half silvered plate and brought together again to give interference bands, there must be a point to point correspondence between the two parts that are brought together. There can, for example, be no appreciable lateral displacement of one beam with respect to the other, otherwise we should in reality be obtaining interference

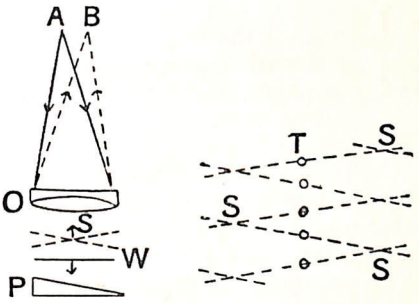

FIG. 5.1.—Fizeau's Localized Fringe Interferometer

effects from light from different sources—the light from one part of the extended source to interfere with that from another part,—which we have seen is impossible in practice.

If a point source A (Fig. 5.1) of monochromatic

radiation be placed at the focal plane of a well-corrected object glass O, the emerging wavefront W is plane, and all parts have the same phase. This is divided by reflection at the two surfaces of a wedge-shaped plate P. If the dotted lines in the inset represent the crests of successive waves from each surface of P, the points such as S where they overlap will correspond to a maximum intensity, while at points such as T we get zero amplitude, since here the crest of one wavefront corresponds to the trough of the other. Thus an eye placed at B will see a maximum intensity in the direction of S and a minimum or dark band corresponding to T. The fringes appear localized at the plate P. The method was first given by Fizeau [1] and the fringes are known as Fizeau fringes. Its practical form which has been developed by Laurent,[2] Lummer,[3] and others is shown diagrammatically in Fig. 5.2. The small aperture at S is slightly displaced from the principal axis of the objective so that the back reflected beams are similarly displaced on the opposite side. For convenience, a right-angled prism is used, so that the eye can be placed at E. The levelling table on which the plate P is laid, has its top blackened to eliminate reflection from its metal top. By this means, localized interference fringes can be obtained with far thicker plates than would be possible with the small aperture method considered in Chapter III. The position and tilt of P are not critical and the method is widely used in optical workshops to test the parallelism of plates. It is actually a test of the constancy of $2\mu t$, and a scale can be placed on the plate so that the number of fringes per unit length is readily obtained. The planeness of a surface can also be tested by having a standard test plate as one surface which can be adjusted parallel

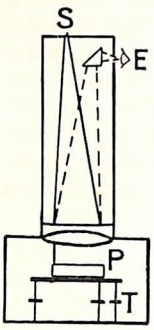

FIG. 5.2.—Interferoscope

to the surface to be tested with the aid of levelling screws. Since we now would have an air plate with constant index any fringes would be due to variations in 't,' i.e. in flatness of the surface under test.

With an air plate one fringe per inch of green mercury light indicates a wedge angle of 2 secs., while with a glass plate it is approximately $\frac{4}{3}$ secs.

It is of course immaterial whether the small aperture is placed at S or at E, since the one stop is the image of the other, for only rays which have passed through S can enter the aperture at E.

Fizeau's apparatus is strictly limited to the testing of parallel or very nearly parallel plates and plane surfaces, while in optical work spherical surfaces and prisms are most frequently needed. Although special methods such as the Hartman [4] test have been developed to test lenses, they are often so highly technical that they necessitate considerable skill in their application.

The extension of Fizeau's principle to the general case of two clearly separated beams (as distinguished from the practically superposed beams in the Fizeau arrangement) by Twyman and Green [5] marks a big forward step in Interferometry and consequently has rendered possible remarkable advances in the perfection of optical instruments.

Twyman and Green's Interferometer

The basic idea is to divide a *plane* wavefront, as given from a point source at the focal plane of a well-corrected objective, by a half silvered mirror. The one beam is reflected back from a plane mirror M_1 and the other from a mirror M_2; either beam may have passed through a plate or prism. On reuniting, the two beams are brought to a focus by a second objective and the *eye is placed at its focal plane.*

When the two reuniting wavefronts are plane the appearance of the field of view will be of uniform colour or intensity, the value depending on the extent to which the wavefronts reinforce each other. If one

of these wavefronts, such as the solid curve in Fig. 5.3, is deformed from the plane formation, either by its passage through a non-uniform plate or due to a defective mirror, the interference bands CD are seen in the field of view. As Twyman [6] has pointed out, these may be regarded as contour lines of the deformed wavefront, the fringes corresponding to different levels, one wavelength apart, of the deformed wavefront.

The interference pattern CD would appear exactly the same if the solid wavefront AB were reversed, i.e. the retardation at A to become a forward displacement

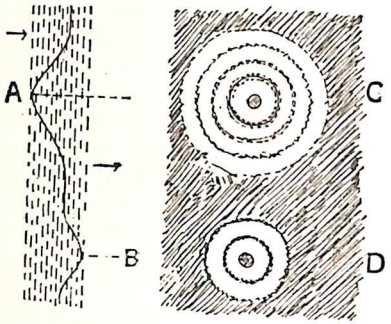

FIG. 5.3.—Distorted wavefront, and Interference pattern obtained with it

of the wavefront. By gently pressing that corner of the interferometer near the mirror reflecting the deformed wavefront, the latter is then slightly retarded with respect to the successive plane waves from the other beam, owing to the increased path. A moves to the left with respect to the dotted lines and therefore the pattern at C opens out. When the deformation is a hill as at B, the same pressure will cause the rings to close in.

Fig. 5.4 shows how the method is adapted to test prisms, and the inset shows how a lens system can be examined. The wavefront W_1 is plane, since we have a point source S at the focal plane of the well-corrected

objective O_1. The plane mirror M_2 is adjusted to reflect the beam emerging from the prism P normally along its own path, so that with a perfect prism, the returning wavefront W_2 would be plane and parallel to W_1. When W_2 and the wavefront back reflected from M_1 are incident on the objective O_2 parallel to each other, an eye placed at E, the focal point of O_2, would observe

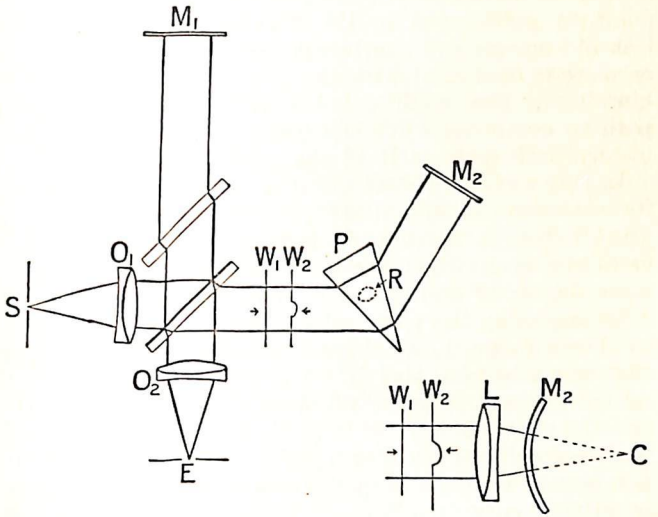

FIG. 5.4.—Twyman and Green's Method of testing prisms and lenses

a field of uniform intensity, while any deformation of W_2 due to the prism P would show up as fringes in the previous figure. The optician then taking a grease pencil can trace these fringes on one surface of P, and after determining whether they correspond to crests or troughs in the wavefront, the prism can be removed and the defects corrected for by local polishing with pencil polishers.

Hitherto, the method of constructing a large prism

had been simply to get the refracting surfaces of the prism plane, as tested by means of a proof plate. Even when this has been done to a very high accuracy the definition of spectral lines through such prisms is often disappointingly poor, so that the advantage of increased resolving power due to sharpness of line image given by theory is lost. This interferometer has shown the trouble to be due to the refractive index varying from point to point even in the best optical glass. This lack of homogeneity can be allowed for when the prism or plate is examined with the interferometer and then 'localized,' the small polisher reducing the metrical path to compensate for the increased refractive index in any part such as R of the prism.

In this way, the construction of large aperture prisms for astronomical and other purposes, which was to a great extent a matter of chance, has now become a certainty even when the glass available has not the same degree of homogeneity as before.

On replacing the plane mirror M_2 by a convex mirror as shown in the inset, the method can be used to test the definition of a lens L. The lens, if perfect, should refract all rays to meet at its focus C; if this point is also the centre of curvature of M_2, the rays are reflected back normally on their own paths and will emerge from L a second time giving a plane wavefront. It is comparatively easy to obtain a truly spherical reflecting mirror, so that any defects showing in the interferometer will be due to the lens L, and can be marked and corrected for as in the case of the prism.

The particular arrangement outlined only permits the axial or central beam to be examined; while this is sufficient for telescope objectives, it is obviously not enough for wide-angled camera lenses. A special type of camera lens interferometer has been designed to accommodate lenses up to $5\frac{1}{2}$ inches aperture and about 30 inches focal length. With this interferometer, the lens under test can be rotated about its second nodal point. As this would displace the focal plane

of the lens from the centre of curvature of the convex mirror a mechanical link arrangement moves the mirror, so that its centre of curvature is always in the focal plane of the lens, independent of the latter's obliquity.

The interpretation of the results obtained, while very easy in the case of plates and prisms, becomes more difficult in lens systems, for the aberrations have hitherto been analysed and classified on the basis of geometrical conceptions of rays. The general appearances of each of the five classes of Seidel [6] have been given by Twyman ; [7] Kingslake [8] has used the simple lens Interferometer both for checking the interferograms expected under definite conditions of tilt, etc., and for comparison with the older method of testing due to Hartmann. The possibilities of the Camera Lens Interferometer have been investigated by T. Smith,[9] and a Universal Lens Interferometer has been developed by him in conjunction with Dowell.[10]

A similar Interferometer, on a smaller scale, has been designed by Twyman [11] to test Microscope objectives. In this case it is not practicable to construct an optical mirror of sufficiently small radius of curvature and of the requisite accuracy, but a tiny drop of clean mercury acts as a practically perfect convex mirror, to reflect the light back through the objective. Owing to its small size the gravitational forces are negligible compared with those of Surface Tension, so that over the essential part the globule is spherical. A whole microscope can thus be tested, but it is more usual to test objectives alone and to include a weak negative lens to compensate for the finite distance of the image from the objective when the latter is used in the microscope. The mercury drop can be dispensed with if two objectives, the one a standard and the other a test objective, are used in series. These are turned towards each other and separated so as to have a common focal plane ; the convex mirror for back reflection may then have a radius of curvature of several inches.

These interferometer methods show objectively the errors that previously could only be deduced by estimation by experienced lens testers. Their greatest utility however will probably be in the development of definitely aspherical surfaces to compensate for the aberrations inherent in wide-angled spherical surfaces.

Other Interferometric methods of testing object glasses have been developed by Waetzmann,[12] Michelson [13] and Ronchi.[14]

Adjustment of Michelson Interferometer

Provided the path lengths are approximately the same, a Michelson Interferometer is in adjustment when the plane of the dividing mirror accurately bisects the angle between the two fully silvered mirrors, and the normals to the surfaces are coplanar. It is not essential that one arm should be at 90° to the other, in fact, if the angle of incidence on the dividing mirror were reduced from 45° to, say, 20° and the positions of the other mirrors altered accordingly, an appreciable saving in the size of the dividing mirror could be effected.

Even when the circular (infinity) Michelson fringes, or the thin plate localized fringes are wanted, they can be obtained very quickly by converting it into the Twyman and Green arrangement with the addition of two objectives and a screen with a small (·5 mm.) aperture as in Fig. 5.4. An opalescent lamp behind the screen gives two back reflected images on the screen, one from each mirror, similarly at the focus of the other objective two images are seen. When the two spots on the screen S coincide at the aperture *simultaneously* with the overlapping of the two spots at E the instrument is in adjustment. This can be rapidly obtained since a tilt of the dividing mirror affects the spot images unequally. On placing the eye at E fine Interference bands are seen when the lamp is replaced by a monochromatic source. These

fringes can be widened by a small tilt of either of the fully silvered mirrors until the whole field is occupied by one or part of one fringe. If the path difference is not too small, the circular fringes are found by removing the screen (so as to have an extended source) and adding an eyepiece at E.

The distinction between the localized fringes in the two arrangements can be readily shown in the following way. The instrument is adjusted for Twyman and Green fringes as mentioned above, but with a path difference of say 1 cm. The fringes are observed through a small (·5 mm.) aperture at E. The first screen and its objective O_1 are consecutively removed without any difference in the appearance of the fringes. [Their presence is immaterial when the aperture E is added, since SO_1 can be regarded as images of EO_2 in the dividing mirror.] On removing O_2 the fringes disappear although we are still left with the small aperture at E which would give localized fringes with a much smaller path difference.

There is an essential distinction between the fringes obtained by Fizeau's method and that of Twyman and Green, which is of very great importance in optical work. A Fizeau fringe means the constancy of $2\mu t$ along that line, so that a plate corrected to give a uniform colour all over, would be one in which the variations in index are exactly compensated for by variations in thickness. The Interferometer, on the other hand, tests the constancy of $2(\mu - 1)t$, and the corrections of t for the same variations in μ as before would be approximately three times greater. In many instruments, for example, the transmission echelon grating, it is constancy of $(\mu - 1)t$ that is required, so that an incident plane wavefront emerges from the plate as a plane wavefront. By carefully plotting the Fizeau and the Twyman and Green interference patterns of a thick plate (about 2 cm.), the point to point variations in refractive index can be determined absolutely to within a few units in the sixth decimal place.

Kösters' Method of Determining Absolute Wavelengths

The Twyman and Green Interferometer was mainly used to measure the small path differences that occur in optical work. Kösters [15] has recently used the same method and arrangement to measure large path differences, and so afford a means of obtaining wavelengths in terms of the standard red cadmium wavelength. An analysis of the method together with values of the wavelengths of the red and yellow Krypton lines to one unit in the fourth decimal place in Ångstroms has been given by Weber.[16]

The fixed mirror of the previously described Inter-

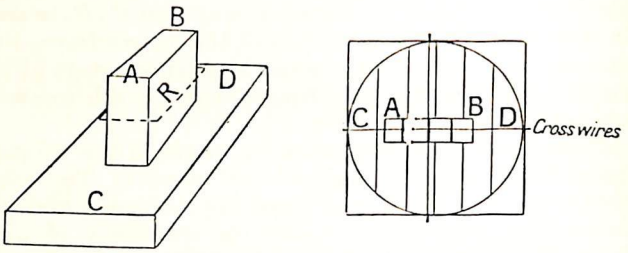

Fig. 5.5.—Mirror unit and Field of View. Kösters' Method

ferometer is replaced by a composite mirror as shown in Fig. 5.5, made up of a distance block or ' end gauge ' placed in contact with the plane CD of the mirror; the block must have its surfaces flat, and AB parallel to the plane CD to a high degree of accuracy. When the other Interferometer mirror is slightly tilted, the appearance of the field of view is as shown in the second part of Fig. 5.5. If the image of this mirror in the dividing mirror comes half-way between AB and CD, i.e. at R, the fringes in both parts are equally clear. Essentially the method is to determine the fraction of the displacement between the two sets of fringes for

three or more known wavelengths, the order of any fringe being as yet unknown; then we have

$$(x_1 + f_1)\ \lambda_1 = (x_2 + f_2)\ \lambda_2 = (x_3 + f_3)\ \lambda_3 = 2\mu t.$$

the fractions f_1, f_2 and f_3 being determined by experiment. The height of the block is obtained within fairly close limits by a micrometer, so that since the beam to the farther mirror CD traverses the path twice, the micrometer measurement gives limits within which the integral values of X_1 must lie. Taking any one of these values, we can work out the *exact* value of t to correspond to it, and with this the units and fractions expected for λ_2 and λ_3. When the calculated fractions for λ_2 and λ_3 agree, for a particular value of x_1 with the observed values, the probability is that the chosen value of x_1 is the correct one. A further check with a fourth wavelength would make it certain. Knowing 't' and the approximate wavelength of another source so that the order of a fringe is known with certainty, a determination of the fractional part enables the wavelength to be known more accurately. The method is exactly the same as that used in wavelength determinations with the Fabry Perot Interferometer (see page 85).

The effect of phase change (page 85) is eliminated when the reflectors AB and CD are of the same metal, and with the reference plane R midway between, the height of the block may be as much as 20 cm. with the more homogeneous Krypton lines. It is claimed that fringe displacements can be determined to within ·01 of the distance between two fringes, so that a relative accuracy of ·0001 Å can be obtained.

Fig 5.6 shows a cross section of Kösters' Interferometer which is manufactured by Carl Zeiss. So that it can be used directly with a source rich in spectral lines without needing an auxiliary spectroscope, a constant deviation (Pellin-Broca) prism P*r* with a drum attachment D immediately follows the cross slit C and the objective O_1. The beam divides at P*b*, part being

reflected to the fixed mirror S_1 and the other part transmitted to S_2 and Q which form a unit similar to that in the previous figure. The beams on reuniting at the half silvered mirror are brought to a focus at B (the focal plane of the second objective O_2), where the eye is placed. Three foot-screws J are used to tilt the table T so that the direction and separation of the fringes can be arranged as desired.

With a given position of the prism, only a very narrow

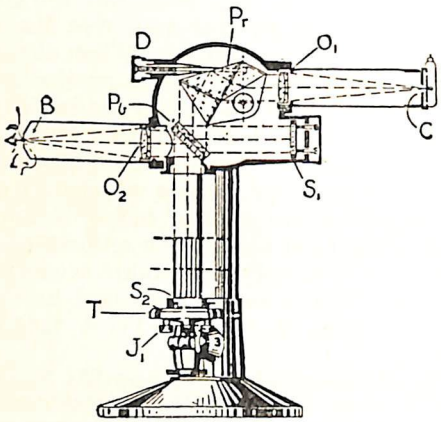

FIG. 5.6.—Kösters' Interference Comparator

spectral region can pass through the aperture at B unless the slit at C is opened in a vertical direction. This would mean that the different parts of the spectrum coming from different parts of the vertical slit C would be superimposed at B. It is thus necessary to determine each fractional part individually, turning the prism drum from one wavelength to the next.

An important application of the instrument is to measure the length in light waves of the case-hardened steel gauges used by engineers in precision work.

The gauge is 'wrung' or pressed against the lower mirror until it adheres to it to form a unit.

Whether the method will replace that of Fabry Perot in the determination of the metre remains to be seen. It does not seem to have been realized that unless the spectral line is symmetrical, the method introduces systematic errors that can be far greater than those of observation, in just the same way as Michelson's Visibility method leads to spurious results when the distribution is unsymmetrical.

GENERAL REFERENCES

V. Ronchi: *La prova dei systemi ottici.* Published by N. Zanichelli, Bologna (1925).
G. Yvon: *Controle des Surfaces Optiques*, Paris (1926).

TEXT REFERENCES

[1] Fizeau: *Comp. Rend.*, **54**, 1237, 1862.
[2] Laurent: *Journ. d. Phys.* (2), **2**, 411, 1883.
[3] Lummer: *Ann. der Phys.*, **23**, 49, 1884.
[4] Hartman: *Zeitschr. f. Instkunde*, **24**, 1, 33, 97 (1904); **29**, 217, 1909.
[5] Twyman and Green: British Patent, No. **103832** (1916); **130224** (1918).
[6] Seidel: cf. Whittaker: *Theory of Optical Instruments* (C.U.P.), 1907.
[7] Twyman: *Phil. Mag.*, **35**, 49, 1918.
[8] Kingslake: *Trans. Optical Soc.*, **27**, 96 (1926); **28**, 1 (1926).
[9] Smith: *Trans. Optical Soc.*, **28**, 104.
[10] Dowell: *Proc. Opt. Conv.*, **2**, 1032, 1926.
[11] Twyman: *Journ. Optical Soc.*, America, **7**, 635 (1923).
[12] Waetzman: *Ann. der Phys.* (4), **39**, 1042, 1912.
[13] Michelson: *Astro. Journ.*, **47**, 283, 1918.
[14] Ronchi: *Rend. Accad. Lincei* (5), **32**, 1, 23, 1924.
[15] Kösters: *Feinmechanik*, 1, 2, 19, 39, 1921; *Zs. für Feinmech.*, **34**, 55, 1926.
[16] Weber: *Phys. Zeitschr.*, **29**, 233, 1928.

CHAPTER VI

INTERFERENCE EFFECTS WITH MORE THAN TWO BEAMS

HITHERTO we have only considered the interference effects between two beams. When a beam of light passes through a transparent plate, multiple reflections occur in the plate. Strictly speaking, these effects ought to have been considered in the case of thin films, but in practice it is sufficient to consider the *first* reflection at each surface, since the successive amplitudes die down so rapidly.

When the reflection coefficient is increased, either by half silvering the plates (method of Fabry and Perot [1]), or by using it at a large incidence angle (method of Herschel [2] and Lummer [3]), the multiple reflections have a profound effect on the character of the fringes ; with monochromatic light, the comparatively broad $\cos^2\theta$ fringes of the Michelson Interferometer or Fresnel Biprism experiment are replaced by very narrow bright fringes on a broad dark background. This action can be understood from the following considerations.

Let AL and BN (Fig. 6.1) be two plane and parallel half silvered films with a separation 't,' placed in front of an objective O whose focal plane is FF^1. Assume that plane wavefronts of wavelength λ fall at all angles on the interferometer. If P and R are the fractions of light intensity transmitted and reflected at each film, the amplitudes are proportional to the square roots of these fractions. Consider a plane wavefront W of unit amplitude making any angle θ with AL, and represented by SA which is normal to W. The amplitude of the part of W transmitted by the first

film (AB) is $P^{\frac{1}{2}}$, and by the second film (BC) is P. Similarly the first reflection at B has an amplitude $P^{\frac{1}{2}}R^{\frac{1}{2}}$, DE is $P^{\frac{1}{2}}R$, so that EG is PR. In the same way the amplitude of the wavefront represented by RU will be PR^2. Each of these wavefronts are plane and parallel so that they will be collected by the objective O at M. There will be a phase difference δ between each train due to the path difference given by:

$$\delta = \left(\frac{2\pi}{\lambda}\right)2\mu t \cos\theta \quad . \quad . \quad . \quad (1)$$

If then the *real* part of $e^{i\omega T}$ represents the incident

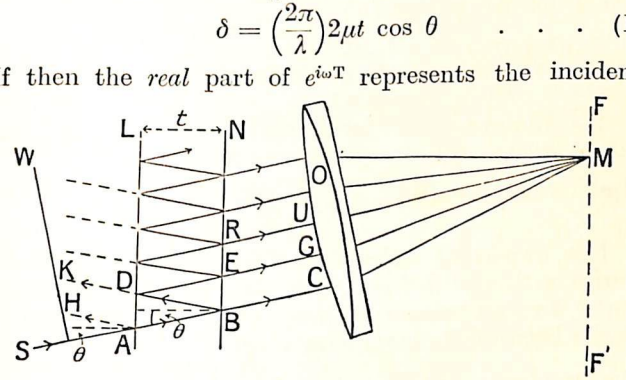

FIG. 6.1.—Formation of Multiple Reflection fringes

light, where $\frac{\omega}{2\pi}$ is the frequency and T the time, the *instantaneous* resultant amplitude will be, from Young's principle, the real part of the sum,

$$Pe^{i\omega T} + PRe^{i(\omega T-\delta)} + PR^2e^{i(\omega T-2\delta)} + \quad . \quad (2)$$

This is: $Pe^{i\omega T}\{1 + Re^{-i\delta} + R^2e^{-2i\delta} + \ldots\}$

$$= \left(\frac{P}{1 - Re^{-i\delta}}\right)e^{i\omega T}.$$

Here, both the amplitude term and $e^{i\omega T}$ are complex; if the former be $(a + ib)$ where both a and b are real, the resultant amplitude is given by $\{a^2 + b^2\}^{\frac{1}{2}}$, for since $e^{i\alpha} = \cos\alpha + i\sin\alpha$, if $r\cos\phi = a$ and $r\sin\phi = b$, then $(a + ib)\,e^{i\omega T} = re^{i(\omega T+\phi)}$ where $r = \{a^2 + b^2\}^{\frac{1}{2}}$ is now a real quantity. Rationalizing the above in this way we have:

$$\frac{P}{(1 - Re^{-i\delta})} = \frac{P}{(1 - R\cos\delta) + iR\sin\delta}$$

$$= \frac{P(1 - R\cos\delta) - iRP\sin\delta}{1 - 2R\cos\delta + R^2}.$$

Thus:

$$a = \frac{P(1 - R\cos\delta)}{1 + 2R\cos\delta + R^2} \quad \text{and } b = \frac{-RP\sin\delta}{1 - 2R\cos\delta + R^2}$$

The Intensity is therefore,

$$a^2 + b^2 = \frac{P^2\{(1 - R\cos\delta)^2 + (R^2\sin^2\delta)\}}{[1 - 2R\cos\delta + R^2]^2}$$

$$= \frac{P^2}{1 - 2R\cos\delta + R^2} = \frac{P^2}{1 + 2R(1 - \cos\delta) - 2R + R^2}$$

$$= \frac{P^2}{(1 - R)^2} \times \frac{1}{1 + \frac{4R}{(1 - R)^2}\sin^2\delta/2} \quad . \quad (3)$$

This important expression shows how the intensity varies with $\sin^2\delta/2$ and with the film properties. As $\sin^2\delta/2$ varies between its limits of 0 and 1, the intensity varies between its maximum value of $P^2/(1 - R)^2$ and the minimum $P^2/(1 - R)^2 \times \left(\frac{1 - R}{1 + R}\right)^2$ or $\frac{P^2}{(1 + R)^2}$.

The visibility or clearness of the fringes:

$V = \frac{I_{max.} - I_{min.}}{I_{max.} + I_{min.}}$ is therefore $V = \frac{2R}{1 + R^2}$ and is independent of the transparency of the films. It is a parabolic curve, with the visibility only increasing from ·8 to 1 as the reflecting power increases from 50 per cent. to 100 per cent.

Resolving Power of Fabry Perot Interferometer

The order n of a fringe is $\frac{2\mu t\cos\theta}{\lambda}$ and it decreases as we go away from the centre, i.e. as θ increases; writing n_0 as the order at the centre where $n_0 = \frac{2\mu t}{\lambda}$ we get by differentiation

$$\frac{\lambda}{\delta\lambda} = -\frac{n_0}{\delta n_0},$$

so that the resolving power for a given n_0 depends on the smallest change of order that can be recognized.

In connection with the spectrum from a diffraction grating Rayleigh's rule is that if the central maximum of one spectral line coincides with the first minimum of another, the double nature of the composite line can just be seen, and the lines are said to be 'resolved.' This resolution is not absolute, it is shown merely as a decrease in the intensity at the centre of an otherwise rather broad line. If the two lines have the same intensity it is easy to show from the theory of a diffraction grating that the intensity at the centre of the saddle portion is $\left(\frac{8}{\pi^2}\right)$ of the maximum of a single line, so that the intensity at the point of overlap for each line is $\frac{4}{\pi^2}$ or ·405.

Although with the development of registering microphotometers such as the Moll,[4] dips much smaller than this can be accurately measured, it is convenient for the purpose of comparison with gratings and echelons to keep to this standard. If A in Fig. 6.2 represents the intensity distribution with n for a wavelength λ, and B for wavelength $\lambda + \delta\lambda$,

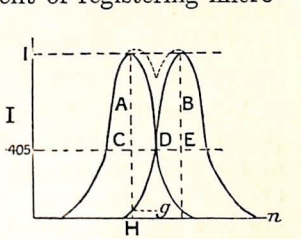

FIG. 6.2.—Resolving Power of Fabry Perot Interferometer

From Eqn. 3

$$I = \frac{I_{max.}}{1 + \frac{4R}{(1-R)^2}\sin^2 \delta/2}, \text{ or writing F for } \frac{4R}{(1-R)^2}$$

$$I = \frac{I_{max.}}{1 + F \sin^2 \delta/2}.$$

$I_D = \cdot 405\ I_C$ under the above conditions, so that:

$$\sin^2 \delta/2 = \frac{1 - \cdot 405}{\cdot 405\ F} = \frac{1 \cdot 469}{F},$$

giving $\delta = 2 \sin^{-1} \sqrt{\frac{1 \cdot 469}{F}}$. This δ is the phase change corresponding to CD in the diagram, so that the phase change for CE will be twice this value. A change of 2π in phase is equivalent to unit change of order since the equation is periodic in this amount.

The total phase change $2\delta = 4 \sin^{-1} \left(\frac{1 \cdot 21}{\sqrt{F}}\right)$ therefore corresponds to an order change $\delta n_0 = \frac{2 \sin^{-1} (1 \cdot 21/F^{\frac{1}{2}})}{\pi}$ and the Resolving Power

$$\frac{\lambda}{\delta\lambda} = -\frac{n_0}{\delta n_0} = -\frac{n_0 \pi}{2 \sin^{-1} \left(\frac{1 \cdot 21}{F^{\frac{1}{2}}}\right)} \quad . \quad (4)$$

When the reflecting power R is high, the value of $F^{\frac{1}{2}}$ is sufficiently large that the angle can be taken for the Sine, and the resolving power becomes:

$$\frac{\lambda^*}{\delta\lambda} = -\frac{n_0 \pi\ F^{\frac{1}{2}}}{2 \times 1 \cdot 21} = -n_0 \left[\frac{\pi R^{\frac{1}{2}}}{1 \cdot 21 (1 - R)}\right] \quad . \quad (5)$$

As shown in Chapter II, page 27, the resolving power of a reflection echelon grating is the product of the order of the spectrum and the total number of apertures, this being true for all types of gratings. On this analogy, the term in square brackets in the above equation can then be called the *Effective Number of Reflections* N_e, thus the resolving power is directly proportional to N_e and proportional to the square root of F which has been called by Fabry *coefficient de finesse*. The manner in which the effective number

* The negative sign for the resolving power as in the corresponding prism formula of Rayleigh is to be neglected since R.P. is essentially a positive quantity. It occurs here simply because a positive change of λ corresponds to a negative change of order δn.

of reflections (and consequently the resolving power) depends on R can be seen from the following table given by the bracketed term in Eq. 5.

Reflecting Power . .	·95	·925	·90	·85	·80	·75
Effective N_e (Eq. 5) .	50·6	33·3	24·6	15·9	11·6	8·9
Closer approx. (Hansen)	58·5	40	29	18·5	13·5	10·5

The third line is from some hitherto unpublished calculations kindly supplied by Dr. G. Hansen, who has made allowance for the increase of the maximum of A (Fig. 6.2) by the addition of the small part GH due to B. When the reflecting power is very low this overlapping is greater and causes a larger percentage change; a close approximation is obtained by adding a sixth to the values calculated from 4. The width of a bright monochromatic fringe is inversely proportional to N_e. It will be seen that a Fabry Perot Interferometer with R = ·90 is equivalent to a reflection echelon grating of 29 plates having the same plate thickness as the spacing of the Interferometer. The plate thickness of the corresponding transmission echelon will be approximately four times greater since the order of the spectrum in this case is $\frac{(\mu-1)t}{\lambda}$ as compared with $\frac{2t}{\lambda}$ in the reflection type.

Unfortunately, high reflection coefficients are only obtainable with the films of pure metals and alloys hitherto examined, in the longer wavelength region. While silver is most generally used for the visible spectrum, gold films give definitely higher reflection coefficients for the same transmission coefficients in the region above 6700 Å. The following table due to Childs [5] shows how the reflecting power of a standard silver film about 40 $\mu\mu$ thickness varies with the wavelength.

Wavelength . .	6500 Å	6000 Å	5500 Å	5000 Å	4500 Å
R	·90	·88	·84	·75	·63

In the extreme violet the reflecting power of the usual silver film is very low with a corresponding widening of the fringes. Nickel, silicon and platinum films are often used; the writer finds that fair results are obtained with silver when the latter is so thickly deposited as to be almost opaque to the eye, the only disadvantage being that an ultra violet standard must then be used for comparison instead of the red cadmium line. The low value of R for a silver film in the violet and near ultraviolet is in a great measure due to the increased transparency in these regions.

As with the echelon, the spectral range over which a Fabry Perot can be used without overlapping of orders varies inversely as the separation of the plates. Writing $\Delta\lambda$ as the difference between two wavelengths such that the n^{th} order of one coincides with the $(n \pm 1)$ order of the other, we have since $\frac{\lambda}{\delta\lambda} = -\frac{n}{\delta n}$, by putting $\delta n = 1$ the corresponding $\delta\lambda$ is the *range*, $\Delta\lambda = \frac{\lambda}{n} = \frac{\lambda^2}{2\mu t}$, while the smallest resolvable wavelength difference $\delta\lambda = \frac{\Delta\lambda}{(N_e)}$ as in the case of an ordinary grating.

This range, which is the maximum wavelength difference that can be examined without an auxiliary dispersion system, is important when dealing with a complex group of fine lines or a single wide line. When only a few fine lines are being examined it may often be possible and even useful to have an order $(n - 1)$ of wavelength $(\lambda + \delta\lambda)$ in between the nth and the $(n + 1)$ order of wavelength λ. The reality of the overlapping can be easily verified by examining the lines with a different separation of the plates.

Wavelength Measurement with the Fabry Perot Interferometer

Two methods have been devised for comparing wavelengths by means of the Fabry Perot Interferometer.

The earlier method, which has been called the *coincidence method*, is briefly as follows. Let λ_s and λ be two wavelengths, the former the greater being accurately known. For a certain separation of the interferometer plates t_1, a fringe of λ_s coincides with a fringe of the unknown wavelength λ. Then $2\mu t_1 \cos\theta = m\lambda_s = n\lambda$.

The separation of the plates is now slowly increased until coincidence is again obtained. In the second case

$$2\mu t_2 \cos\theta = (m + p)\ \lambda_s = (n + p + 1)\ \lambda,$$

from which we obtain $\lambda - \lambda_s = \frac{\lambda}{p} = \frac{\lambda_s}{(p+1)}$. p can be determined either by actual counting, or by having the mirror separation controlled by a fine micrometer screw, when coincidence of inner rings is observed $\cos\theta = 1$ and $2\mu\ (t_2 - t_1) = p\lambda_s$, from which p is found and the wavelength difference $\lambda_s - \lambda$ determined.

If the wavelengths are widely different, coincidences appear frequently and p becomes small; it is then expedient to determine the positions of several coincidences. In addition to a micrometer screw, the method necessitates the use of very carefully optically worked 'ways' or grooves since the mirrors must retain their parallelism as the separation is varied. The most serious objection to the method is that it involves individual measurements for each line so that it becomes practically an impossibility with a rich or many lined spectrum such as the Iron arc.

Method of Exact Fractions

This method, which is due to Benoit,[6] enables intercomparison of wavelengths to be easily and rapidly made and is very largely responsible for the importance of the Interferometer in modern Spectroscopy.

Our standard wavelength is that of red cadmium in dry air at 15° C., and 760 mm. pressure, 'g' being 980·67 (at latitude 45°). This is taken to be 6438·4696 Ångstroms, so that probably this unit differs but very slightly from the tenth metre (10^{-10} metre). If λ_s and

λ_m denote the wavelengths in vacuum and in a medium of index μ, of a radiation of frequency ν, $\nu\lambda_v = C$ where C is the velocity of light in vacuum, and $\nu\lambda_m = V$, V being the velocity in the medium. Hence $\frac{\lambda_v}{\lambda_m} = \frac{C}{V} = \mu$. The optical path difference $2\mu t \cos\theta$ is an integer number of wavelengths (measured in vacuo) so that $2t \cos\theta = n\lambda_m$ is the fundamental equation for reinforcement in the medium.

In general, the order at the centre $n_0 = \frac{2t}{\lambda}$ is not an exact integer, it will generally be an integer n_1 (which is the order of the first bright ring) + a fractional part ε_1, so that the equation becomes $n = n_0 \cos\theta = n_0 \cos\phi/2$. ϕ is now the angular diameter, and this is usually small, so that we can write

$$n = n_0\left(1 - \frac{\phi^2}{8}\right) \text{ or } \phi = \sqrt{\frac{8}{n_0}} \cdot \sqrt{n_0 - n}.$$

For the first bright ring, $n_1 = n_0 - \varepsilon_1$ so that its angular diameter $\phi_1 = \sqrt{\frac{8}{n_0}}\sqrt{\varepsilon_1}$, for the second ring, $n_2 = (n_0 - 1 - \varepsilon_1)$ and $\phi_2 = \sqrt{\frac{8}{n_0}} \cdot \sqrt{\varepsilon_1 + 1}$, and similarly for the pth ring,

$$\phi_p = \sqrt{\frac{8}{n_0}} \cdot \sqrt{\varepsilon_1 + (p - 1)}.$$

The linear diameters of the various rings at the focal plane of an objective is given by multiplying these values by its focal length. The fringes are similar to those in Newton's rings in that the diameters of successive rings increase approximately as the roots of integers, but with this difference that the order number decreases as the ring diameter increases, the contrary being the case with Newton's Rings. For any excess fraction ε the diameter of the first ring varies inversely as $n_0^{\frac{1}{2}}$ so

that the size of a ring with a plate separation of ·25 cm. is twice that for a gap of 1 cm.

Calculation of wave-length.

The exact value of the separation is first determined in the following manner. The interferometer is placed in the parallel beam of a spectrograph, or the interference rings are focussed on the slit by an auxiliary objective. A photograph is then taken using a source containing three or more accurately known wavelengths, and the diameter of, say, the third ring for each wavelength is measured with a photomeasuring micrometer. When the Fabry Perot is in the parallel beam, the focal length of the camera objective is required to within about 1 per cent. and the actual diameter of the third ring $d_3 = \phi_3 f = \sqrt{\frac{8}{n_0}}\sqrt{\varepsilon+2}\, f$. An approximate value of n_0 enables the fraction ε to be determined. The other fractions are determined in the same way. Although the diameter of the inner ring will give ε more quickly it is not advisable to use this as near the centre the *dispersion* $\frac{d\theta}{d\lambda}$ increases very rapidly. The subsequent procedure can best be illustrated by an example. A Fabry Perot of separation 10·040 mm. (approx.) gave the following fractional parts with the following accurately known lines:

Wavelength	6096·163 (Ne.)	5852·488 (Ne.)	5015·679 (He.)
Fractional Parts	·20	·90	·35

The value of n_λ for λ 6096 must therefore be in the neighbourhood of 32941, actually $(n_0)_{\lambda 1} = 32941{\cdot}20 \pm \mathrm{x}_1$ where x_1 is an integer. For the second line $(n_0)_{\lambda 2} = (n_0)_{\lambda 1} \times \frac{\lambda_1}{\lambda_2}$. Thus for different values of x_1 we can calculate the order and the fractional part for λ_2 and similarly for λ_3. The value of x_1 that gives the correct fractional part for both λ_2 and λ_3 must then be a possible one.

Assumed order (n_0) for	Corresponding orders calculated for	
6096 Å	5852 Å	5015 Å
32943·20	34314·82	40039·90
32944·20	34315·87	40041·11
32945·20	34316·91	40042·32
32946·20	34317·95	40043·54

It is thus clear that the appropriate order for 6096 Å is 32945·20, giving a value of $t = 10{\cdot}04197$ mm. The three lines give agreement of fractional parts again when $t = 10{\cdot}049$ mm., but it is assumed that this separation is ruled out by the preliminary micrometer determination of t. In any case all ambiguity is removed by a check with a fourth accurately known line.

The wavelength of a line to be measured must be previously known with sufficient accuracy that the order can be calculated to within one unit. In the above example the order for $\lambda = 5000$ Å is approximately 40,000 so the wavelength must be known to well within ·1 Å, the interferometer determination enables the probable error to be reduced to about ·002 Å with sharp lines. With a 10 cm. plate separation the preliminary value must be known to within ·01 Å, while only provided the line is sufficiently monochromatic so that the fringes still remain sharp, can the probable error be further reduced to about ·0002 Å. In practice this is rarely possible.

When using large separations, constancy of temperature and, even more important, of atmospheric pressure are essential. An increase of ·2 mm. (Hg.) in atmospheric pressure increases the order of interference in a 6·25 cm. interferometer (λ 6438 Å) by ·015, an amount that can be easily detected, so that long exposures, even in constant temperature rooms, are only practicable in settled weather conditions.

If the light source is focussed on the interferometer each point of the source contributes to form each part

of the fringe system. The wavelengths thus found are the mean wavelengths of the source; when the source and the fringes are simultaneously focussed on the slit, or the interferometer is placed in the parallel beam of the spectrograph, this is not the case. Here any particular part of the fringe pattern originates solely from a particular part of the source so that any small local variation of the wavelength will show up as a deformation of the fringe. It should be possible by this method to investigate the electric fields in arcs and particularly striations in Geissler tube discharges. In wavelength measurements, it is customary to focus the light source on the interferometer whose aperture must, as Buisson and Fabry have pointed out, be limited so that the beam is smaller than the prism or grating of the auxiliary dispersing spectograph. It would appear that more accurate values might be obtained with the other method if the relatively narrowest and least disturbed portions of fringes be selected for measurement.

A small phase change occurs at metallic reflection which in effect makes the separation of the plates virtually greater. It can be determined by finding the exact fractions for two different separations. When the same wavelengths are used the discrepancies in the fractional parts give the variation of this phase change with wavelength. Fortunately its variation with wavelength is small, and its effect decreases with increasing plate separation. It can be compensated for by subtracting the following amounts from the observed orders:

6500 Å	6000 Å	5500 Å	5000 Å	4500 Å	4000 Å
·0	·002	·005	·011	·023	·045

The above values give the corrections for a cathodically sputtered silver reflector; they vary slightly with different films; full details of methods of evaluating them are given by Meggers.[7]

One point needs to be emphasized. If a wavelength is determined by using the secondary Iron Arc standards in its neighbourhood to calculate the separation, the

phase change is automatically compensated. In addition, if the determinations are *not* made at the normal conditions (15° C. 760 mm. pressure) the wavelength obtained will be its wavelength at 15° C. and 760 mm. This also applies to prism and grating measurements since the standard wavelengths are altered by practically the same amount.

If a line in the violet is to be compared directly with the red cadmium, then both the phase correction and actual temperature and pressure conditions become important. The Bureau of Standards [8] has published data of the refractive index of air for wavelengths from 2,200 Å to 9,000 Å at various temperatures and pressures, obtained by determining the change of order on evacuating an interferometer in a constant temperature bath. Correction tables have been calculated for use when observations are not made under the normal conditions and for obtaining the wavelength in vacuum as required for theoretical ' series ' calculations.

Two Fabry Perot Interferometers in Series (Brewster Fringes)

When the separation of one interferometer is the same as or is an exact multiple of that of the other, the Brewster fringes (see Chapter III, page 41) are obtained when the interferometers are slightly inclined. Since the intensities of successive reflections decrease in a geometrical series, the visibility or the clearness of these fringes decrease as the ratio of the separation increases. With a 1 : 4 separation ratio, for example, the fringes seen are due to interference between one reflection at the thicker interferometer and four at the other, or between two multiple reflections at the first and eight at the second ; as the ratio increases their amplitude difference becomes more apparent and the interference fringes less distinct.

The constancy of pitch of a micrometer screw can be tested by this method. A fixed separation interferometer (Etalon) is placed in series with a variable

separation interferometer whose separation can be accurately controlled and measured by means of the screw under test. The separation is adjusted until it equals that of the Etalon, when the Brewster white light fringes will appear if the two systems are not exactly parallel. The reading is taken, and the variable gap increased to twice three times, etc., the Etalon separation when the white light fringes will again appear. The ratio can be increased to about 10 or 12 before the fringes become too indistinct for measurement. Alternately, the separation of the interferometer can be reduced to $\frac{1}{2}$, $\frac{1}{3}$, etc., of that of the fixed Etalon. The 'ways' or grooves along which the movable mirror moves must be made with such accuracy that the interferometer plates always remain parallel to within about 1 second of arc.

These superposition fringes, in contradistinction to the Fabry Perot fringes, are comparatively broad, and are similar to the Michelson and Jamin interferometer fringes.

Benoit, Fabry and Perot's determination of the Metre [9]

These Brewster fringes formed with Fabry Perot interferometers of unequal separation were first described by Perot and Fabry [10] in 1899. Fourteen years later, in conjunction with Benoit the method was used to determine the number of waves of red cadmium in the standard metre. Five Etalons were constructed with U-shaped separators of invar steel and arranged in line as shown in Fig. 6.3, their lengths being 100, 50, 25, 12·5 and 6·25 cm. As in the Michelson experiment the procedure involves three distinct experiments.

(I) The determination of the number of cadmium waves in the shortest Etalon E.

(II) The intercomparison of the successive sub-standards.

(III) Comparison of the 100 cm. Etalon with the copy R of the Prototype metre.

The first is effected once and for all by the method

of exact fractions discussed on page 85. This establishes the order of interference and the telescope T is used to determine the actual fraction at the time and under the condition of the experiment. No attempt was made to get one substandard exactly twice the next, the half silvered air wedges F and G which give localized fringes were calibrated for red cadmium light from S reflected by mirrors 14 and 16, or 14 and 15, and used to compensate for this difference. By a suitable choice of mirrors any pair of successive Etalons can be compared *in situ*. Thus to compare C and D the mirrors

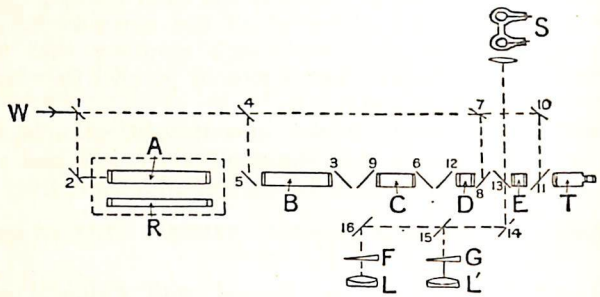

FIG. 6.3.—Benoit Fabry and Perot Determination of the metre

1, 4, 6, 12, are moved out of the way so that the white light beam from W is reflected at 7, 8, and 9 to the viewing lens L, focussed on the wedge F. The displacement of the central fringe in the wedge is a measure of 2D — C, where C and D are the lengths of the corresponding Etalons.

Instead of attempting to set the travelling microscopes on the edges of the plates of A when comparing it with the metre R, the measurements were made to rulings on the edges of the plates (close to the surface) similar to those on R. The distances from these rulings to the effective reflecting surfaces were then found by mounting the actual plates of A to form first a 1 cm. and then a 2 cm. Etalon, the exact optical thicknesses of which were

determined by the exact fraction method. A straight bar having rulings A, B, C (Fig. 6.4) so that AB $\doteq$ BC $\doteq l_1$ (very closely) is used for comparison by means of the comparator, so that

$$l_1 = \text{AB} + \alpha = \text{BC} + \beta \text{ and } l_2 = \text{AC} + \gamma,$$

the quantities α, β, γ, being of the order of a few microns (10^{-3} mm.) only. If X is the sum of the distances (measured in wavelengths) of each mark from the reflecting surface, $l_1 = (\text{M}_1 + \text{X})\,\lambda$, $l_2 = (\text{M}_2 + \text{X})\,\lambda$ where M_1 and M_2 are the optical separations already determined; eliminating l_1 and l_2 we have

$$\text{X} = \text{M}_2 - 2\text{M}_1 + (\alpha + \beta - \gamma)\,\lambda^{-1}.$$

The principal advantage of this over the earlier method of Michelson is that all the material observations for a complete determination can be carried out in a few hours while conditions of pressure and temperature are constant. The number of wavelengths in a 6·25 cm. Fabry Perot Etalon can be determined with greater accuracy than the number in a 10 cm. Michelson substandard, and in this newer method only four intercomparisons are required. The number of wavelengths of red cadmium radiation in a metre of *dry* air at 15° C. and 760 mm. pressure was found to be 1,553,164·13, so that the wavelength of the cadmium line is

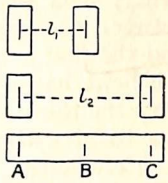

FIG. 6.4.—Determination of End Correction

$$6438{\cdot}4696 \text{ Å or } 10^{-10} \text{ metres}$$

with an estimated probable error of $\pm$ ·0005 Å. This value is in close agreement with Michelson's determination, when a correction is made for the effect of an average amount of water vapour (no account of it was taken in the earlier experiment).

Two Fabry Perot Interferometers in Series

Although the theory of two interferometers in series was worked out by Perot and Fabry in 1899,[11] it is

only in the last few years that the method has been employed for the fine structure analysis of spectral lines.

In the superposition fringes discussed above, the two Etalons are slightly tilted with respect to one another ; the fringes are straight lines, and can be obtained with white light. In this method, the superposition fringes disappear, being infinitely wide when the Etalons are exactly parallel.

When two identical Etalons or Fabry Perot Interferometers are placed in series and are parallel, it can be shown that the resolving power of the combination is some 60 per cent. greater than that of either instrument used alone. This is when the distance between the two is such that no interference effects are obtained between the second surface of the one interferometer and the first surface of the other. On the other hand, the light has now to pass through four half silvered films the thicknesses of which have to be considerably less to give the same transparency as with a single interferometer. This in turn causes a reduction in the reflecting power, so that the resolving power of each unit is considerably reduced. Thus the nett gain may be negligible. It appears that in the red, where a very high value of R can be obtained, it is better to use a single heavily silvered unit, while at the violet end where R is low (coupled with fairly high transparency) the compound interferometer should yield better results.

The main advantage of the method is obtained when the two interferometers are of unequal separation. Suppose we have two such interferometers, the separation of the first being exactly three times that of the second. From the fundamental equation for a maximum bright fringe $2t \cos \theta = n\lambda$, we get for the dispersion $\frac{d\ (\cos \theta)}{d\lambda} = \frac{n}{2t} = \frac{\cos \theta}{\lambda}$, *independent of* t, while the angular distance between the orders $\frac{d\ (\cos \theta)}{dn} = \frac{\lambda}{2t}$ is inversely proportional to t. If θ_1 θ_2 θ_3, etc., are the angular diameters of the bright fringes from the thicker

interferometer, only light making these angles falls on the second. If θ_1 also satisfies the fundamental equation for the second interferometer then we have a bright fringe corresponding to this direction. The next bright fringe of the second interferometer will be θ_4, roughly three times the distance between the fringes of the thicker interferometer. Thus we have a resolving power slightly greater than that of the thicker interferometer, with the increased range without overlapping of orders due to the presence of the thinner interferometer. The disadvantage of the method is that with a low value of R, the intensity in the gap between two maxima for a single interferometer is not zero, so that the suppression of the intervening maxima of the thicker Fabry Perot is not complete. This is shown in the intensity curve of Fig. 6.5. A and B correspond to the real maxima (for both interferometers) for θ_1 and θ_4. C and D are weaker maxima that are maxima for the thicker interferometer only. These spurious maxima may hide weak satellites of the main line so that the true range is not that given by AB.

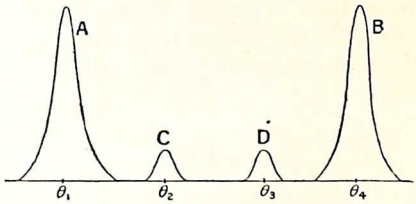

FIG. 6.5.—Fringe Intensity Curves for double Interferometer

Houston [12] at Pasadena has used the method for examining the fine structure of Helium lines, with air spaced interferometers. Gehrcke and Lau [13] at the Reichanstalt employ two half-silvered plane parallel plates of glass of the same melting but of different thickness. The low reflecting coefficient of a silver-glass film (as compared with silver-air) is to a great extent compensated for by the ease of adjustment. This arrangement, owing to the dispersion of glass, can only be used for fine structure work.

Lummer Plate

A high reflection coefficient can be obtained with an unsilvered plate when the light is reflected in the material at nearly the critical angle. This is the basis of the method devised by Lummer [14] and developed by him afterwards in conjunction with Gehrcke.[15]

There are two ways of using a plane parallel plate to obtain high order interference fringes. A concentrated beam of monochromatic light incident obliquely on such a plate will give a series of nearly straight fringes at the focal plane of an objective following the plate. These fringes are almost exactly similar to those from a tilted Fabry-Perot Interferometer, the only difference being that with the latter the dispersion of air is negligible. The patterns on either side of the

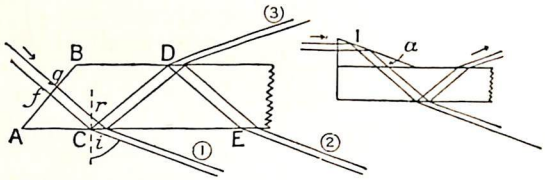

Fig. 6.6.—Methods of passing light into a Lummer Plate

plate are complementary as with Newton's Rings, the fine bright fringes on a dark background observed by transmission are fine dark bands on a light background by reflection. This method is unsatisfactory for two reasons; not only is the amount of light that enters the plate small, but also the *areas* of the successive emergent wavefronts decrease due to the lateral displacement. This in effect is equivalent to reducing the reflection coefficient and hence the resolving power is lowered.

The method adopted is to pass the light into the plate as shown in Fig. 6.6. The incident light enters the plate approximately normal to AB, so that there is a minimum loss of light. The greater part of the light is reflected at C, but a small amount emerges along (1).

Further reflections occur at D and E. For the sake of clearness the incident beam has been limited to *fg*, whereas in practice it would fill the aperture AB. With this method the beams (1) and (2) etc. are deviated; the addition of a totally reflecting prism T makes the plate into a ' direct vision ' instrument when the value of α is suitably chosen. If the successive emergent beams (1), (2) etc., which are parallel, are brought to a common focus by an objective O (Fig. 6.7) the beams will reinforce and produce a bright fringe. The patterns PQR come from the upper side of the plate, and P'Q'R'

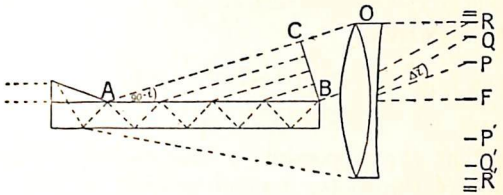

FIG. 6.7.—Formation of Lummer Fringes

from the lower. The two sets are now identical, and not complementary as with the Fabry Perot.

If ' t ' is the thickness of the plate of refractive index μ for a wavelength λ, the fundamental condition for reinforcement is :

$$2\mu t \cos r = n\lambda \quad . \quad . \quad . \quad . \quad (1)$$

Since $\sin i = \mu \sin r$, this can be written:

$$2t \sqrt{\mu^2 - \sin^2 i} = n\lambda \quad . \quad . \quad . \quad (1A)$$

If Δi is the angle between successive orders, we get by squaring and differentiating (1A),

$$n\lambda^2 \Delta n = -2t^2 \sin 2i . \Delta i$$

giving :

$$\Delta i = -\frac{n\lambda^2}{2t^2 \sin 2i} \Delta n.$$

Putting $\Delta n = 1$, we get the angle between successive fringes.

$$\Delta i = -\frac{n\lambda^2}{2t^2 \sin 2i} = -\frac{\lambda\sqrt{\mu^2 - \sin^2 i}}{t \sin 2i} \quad . \quad (2)$$

This shows that the separation, while independent of the length of the plate, increases with wavelength and approaching grazing emergence, and varies inversely as the thickness of the plate.

The *Dispersion* is obtained by differentiating (1A) with respect to λ, remembering that the refractive index is now variable.

$$n^2\lambda = 2t^2\left(2\mu\,\frac{\partial\mu}{\partial\lambda} - \sin 2i\,\frac{\partial i}{\partial\lambda}\right).$$

$$\frac{\partial i}{\partial\lambda} = \frac{4t^2\mu\,\dfrac{\partial\mu}{\partial\lambda} - n^2\lambda}{2t^2\sin 2i} \quad . \quad . \quad . \quad (3A)$$

This may be written,

$$\frac{\partial i}{\partial\lambda} = \frac{2\lambda\mu\,\dfrac{\partial\mu}{\partial\lambda} - 2(\mu^2 - \sin^2 i)}{\lambda\sin 2i} \quad . \quad . \quad (3B)$$

showing that the dispersion is independent of the size and shape of the plate, depending only on the optical properties of the plate, the wavelength, and the angle of emergence.

If we make the Δi obtained from (3A) equal to the Δi of equation (2), the resulting $\Delta\lambda$ will then be the *range* of the plate without overlap, or more strictly, $\Delta\lambda$ is then the difference of wavelength which a component line in any order must have so that it coincides with the main fringe of the next order.

Rewriting (3A)

$$\Delta i = \frac{\left(4t^2\mu\,\dfrac{\partial\mu}{\partial\lambda} - n^2\lambda\right)}{2t^2\sin 2i}\,\Delta\lambda = -\,\frac{n\lambda^2}{2t^2\sin 2i}$$

$$\therefore\ \Delta\lambda = \frac{n\lambda^2}{n^2\lambda - 4t^2\mu\,\dfrac{\partial\mu}{\partial\lambda}} \quad . \quad . \quad . \quad (4)$$

This now famous expression, due to von Bayer,[16] takes into account the effect of Dispersion, and would hold equally well for a Fabry-Perot Interferometer

consisting of a plane parallel glass plate half silvered on both surfaces.

Referring to Fig. 6.7, the width of the beam or wavefront BC entering the telescope is AB cos $i = l \cos i$, l being the length of the plate. The angle δi between the central maximum and the first minimum of a beam of this width is $\left(\frac{\lambda}{l \cos i}\right)$; this is also according to Rayleigh's criterion the smallest angle resolvable. Rearranging Eq. (3B):

$$\delta i = -\frac{1}{\lambda \sin i \cos i}\left\{\mu^2 - \sin^2 i - \lambda\mu \frac{\partial\mu}{\partial\lambda}\right\}\delta\lambda$$

Making $\delta i = \frac{\lambda}{l \cos i}$, the corresponding $\delta\lambda$ will be the smallest wavelength change resolvable.

Resolving power

$$\frac{\lambda}{\delta\lambda} = \frac{l}{\lambda \sin i}\left\{\mu^2 - \sin^2 i - \lambda\mu \frac{\partial\mu}{\partial\lambda}\right\} \quad . \quad (5)$$

This value is only strictly correct at grazing emergence since $\delta i = \frac{\lambda}{l \cos i}$ only when the amplitude is uniform over the wavefront BC. We get a sufficiently close approximation to the limit of resolving power by writing $\sin i = 1$ and $\frac{\lambda}{\delta\lambda} \simeq \frac{l}{\lambda}(\mu^2 - 1)$, so that roughly the R.P. is between 1·4 times and twice the metrical length of the plate measured in wavelengths (the dispersion factor term involving $\frac{\partial\mu}{\partial\lambda}$ only makes a correction of the order of 5 to 10 per cent.).

In practice this grazing emergence is not possible and an exact calculation of the resolving power is complicated by the fact that the decreasing series to be summed is not an infinite one as with the Fabry-Perot Interferometer. If the resolving power given in

(5) is divided by $\left(\frac{l}{2t \tan r}\right)$, the possible number of reflected beams, the dividend $\left(n - \frac{2t}{\cos r}\frac{\partial\mu}{\partial\lambda}\right)$ is the equivalent order of interference. The latter quantity multiplied by the effective number of beams Ne would then be the actual resolving power. Hansen has calculated this value for different plates in terms of the reflection coefficients obtained at different emergence angles. From the Fresnel reflection formulæ we have the reflection coefficient when the magnetic vector is in the plane of incidence $R = \frac{\sin^2 (i - r)}{\sin^2 (i + r)}$ while for the perpendicularly polarized beam the tangent formula holds. Since the Sine formula gives the higher coefficient for a given i, this should always be chosen in practical work by using a Nicol prism. With a quartz Lummer plate following a collimator, a suitable length of slit will enable the two patterns (for the ordinary and extraordinary rays) to be separated without any polarizing device.

Hansen's values are given graphically in Fig. 6.8. With a plate of index 1·5 the calculated reflection coefficients (R) for emergence angles for each degree from 89° to 85° are ·946, ·885, ·829, ·778 and ·731 respectively. With an index of 1·6 the values are slightly higher, thus for 88° the coefficient is ·894. If our plate is 130 × 4·5 mms. the maximum number of reflected beams is about 15, so that curve B in the graph is the appropriate one. When R = ·75 (corresponding to an emergence angle between 85° and 86°) the effective number of reflections (Ne) = 10. Curve A corresponds either to an infinitely long Lummer plate, or to the central fringes of a Fabry Perot. We see that with R = ·75 the resolving power is independent of the length of the plate provided it is sufficiently long to have a possible N = 15. As the tilt is altered to vary R, Ne increases slowly to its possible

maximum 15 when the intensity becomes vanishingly small. A longer plate (N = 30) can be used with R = ·86 giving an effective Ne = 20 without any appreciable loss of light at the end of the plate, since up to this point it coincides with the curve A.

We can therefore make the following generalization. For each plate there is a definite value of emergence

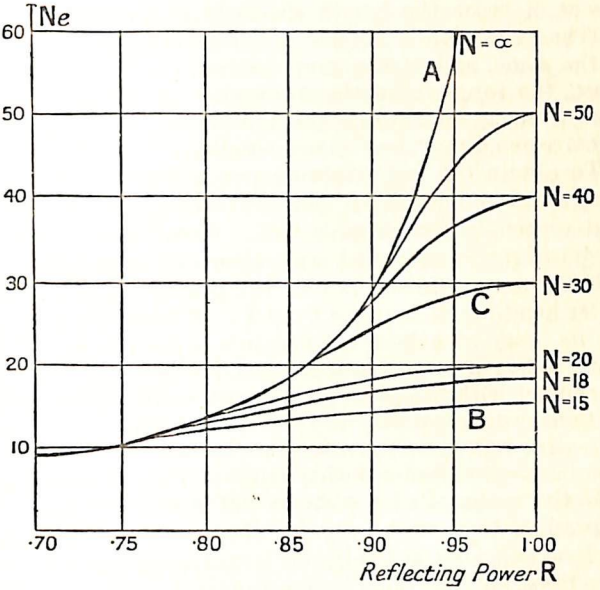

FIG. 6.8.—Effective Number of Reflections (Ne), and Reflecting Power for Fabry Perot (A) and Lummer Plates B, C, etc.

angle (corresponding to a definite R) at which sensibly all the incident light emerges to form the fringe system. The effective number of reflections (Ne) at this angle is approximately two-thirds of the maximum possible; hence the resolving power is two-thirds of the value calculated in Eq. (5), or very closely $\frac{2}{3}\frac{l}{\lambda}(\mu^2 - 1)$.

As a rough estimate the Resolving Power under practical working conditions is from ·9 to 1·3 times the metrical length of the plate measured in wavelengths. It is interesting to compare it with other high resolving power methods. The transmission echelon has a resolving power of $(\mu - 1) \times$ length of the pile of plates, or practically half the length of the pile measured in wavelengths. The Reflection instrument has a power of twice the length similarly measured.

When the plate thickness of the transmission echelon is the same, and of the same material as the Lummer plate, the range $\Delta\lambda$ without overlap of the echelon is four times greater while the 'order' of the spectrum is correspondingly four times smaller.

To obtain the full resolving power from a well-constructed Lummer plate, the surfaces must be clean, and especially free from grease. Great care must be exercised in cleaning as any appreciable pressure in rubbing may seriously impair the definition of a plate. After handling, it requires from 1 to 4 hours (depending on its size) to attain temperature equilibrium before use. When a large plate is used horizontally, the air in contact with the plate may occasionally tend to form stationary layers of slightly different temperature (and refractive index). A gentle draught from a distant fan is sufficient to eliminate this cause of poor definition.

If the material of a plate is not homogeneous, it is impossible to correct fully for the variations in index by local polishing, as the beams traverse the plate in two directions, so that only a compromise can be effected. Quartz plates are superior not only on account of greater homogeneity but also because quartz has a thermal conductivity approximately twenty times greater than glass, and temperature equilibrium is much more rapidly attained.

Crossed Lummer Plates.

The high order, and consequent low range of a plate makes overlapping of orders very common with this

instrument. If a very thin plate be used so that the 'range' is resolvable by the auxiliary prism or grating spectroscope, two difficulties arise. It is extremely difficult to manufacture a long thin plate of the required precision owing to flexure; if such a plate were possible, only a small amount of light could enter because of its small aperture. In consequence the solution is to place the plates in series, with their dispersions crossed. A point source is obtained with a double (cross) slit and the thinner and generally narrower plate placed first. With this arrangement, not only are false lines (ghosts) due to any plate imperfections easily recognized, but it is possible to decide whether a satellite lies on the longer or shorter wavelength side of a main line. The resultant resolving power is slightly higher, and with a proper selection of plate thickness overlapping of orders is eliminated. A detailed account of the method will be found in Section B of the (1929) Catalogue of Adam Hilger Ltd.

Wedge-shaped Lummer Plates.[17]

If instead of being strictly parallel, the plate has a wedge angle of a few seconds of arc, the fringes instead of being at infinity become localized near the plate and can be observed with an eyepiece alone instead of a telescope. Unfortunately, only a few of the successive beams meet approximately at a point and the fringes in consequence are rather broad, and of no particular use.

Miscellaneous Applications of Multiple Reflection Fringes

Channelled Spectra.

When a very thin parallel air plate formed between two half-silvered plates is placed in the path of a white light beam entering a spectroscope, the spectrum is found to be crossed by a large number of dark bands. These fringes, first observed by Fizeau and Foucault,[18] were used by Esselbach [19] and later by Edser and Butler [20] (by which latter name the bands are generally

known in England) to calibrate a spectroscope, and thus to measure wavelengths.

If D is the path difference between a ray that passes through directly and the ray that suffers one reflection, then, when $D = n\lambda$, we have bright fringes. Let $\lambda_0, \lambda_1, \lambda_2$, be the wavelengths of successive bright fringes ($\lambda_0 > \lambda_1 > \lambda_2$); if n_0 is the order of interference for λ_0 that for λ_1 must be $n_0 + 1$.

$$D = n_0\lambda_0 = (n_0 + 1)\ \lambda_1 = (n_0 + 2)\ \lambda_2.$$

$$(\lambda_0 - \lambda_1) = \frac{\lambda_1}{n_0} = \frac{\lambda_1\lambda_0}{D}$$

$$\therefore \frac{\lambda_0 - \lambda_1}{\lambda_0\lambda_1} = \frac{1}{D} \quad \text{or} \quad \frac{1}{\lambda_1} - \frac{1}{\lambda_0} = \text{constant}.$$

This means that the fringes are those of constant frequency difference and can be used to calibrate a spectroscope, for if we have say x fringes between two known wavelengths λ_a, λ_b; then $\frac{\lambda_a - \lambda_b}{\lambda_a\lambda_b} = \frac{x}{D}$ from which D can be found for the particular plate used. With a thin plate, its position is immaterial; it functions equally well when placed between the eye and the eyepiece as in its more orthodox position near the slit.

When the dispersion and resolving power of the spectroscope are high, and the plate separation for fine channelled fringes becomes large, the appearance becomes more complicated. The successive rings of the Fabry Perot now come into action when the plate is in the parallel beam or when the rings are focussed on the slit. The effects have been studied by Gehrcke and Reichenheim [21] and by Burns.[22] For a given separation, there is an optimum slit width for best visibility of fringes.

Astrophysical Applications of Multiple Reflection Fringes

In 1914 Buisson, Fabry and Bourget [23] used a Fabry Perot to investigate the nature of the emitter of the

3727 and 5006 'Nebulium' lines which are given by the great nebula in Orion but have not been terrestrially observed. The interferometer was mounted after the eyepiece of an 80 cm. diameter reflecting telescope. Another object glass following the plates focussed both the image of the nebula and the fringe system on a photographic plate. The other few lines of its spectrum were absorbed by filters. By determining the limiting path difference over which fringes could be seen for these lines as compared with the value for the hydrogen lines present in the Nebula they concluded that the mass of the emitter was 3 (Hydrogen = 1). The circular ring system was deformed in parts showing local Doppler effect due to a relative motion (in the line of sight) of different parts of the Nebula.

A somewhat similar experiment has recently been tried by the writer [24] of combining a Fabry Perot interferometer with a spectroheliograph. This latter instrument is essentially a spectroscope with an additional slit at the focal plane of the telescope lens. The photographic plate immediately following the second slit and the solar image are fixed, while the remainder of the apparatus can move laterally. This motion will give a picture of the sun in one wavelength. If now a Fabry Perot be placed in the parallel beam in front of the prism, the image at the second slit becomes a series of fringes, very short arcs of the ring system. The pattern therefore from a strictly constant wavelength source would be straight line fringes. Local variations due to Doppler and other effects show up as local deformations of the straight line fringes, which are not true interference bands but are a synthetic building up of Fabry-Perot ring sections due to the motion of the Spectroheliograph. It is probable that the method could also be used to investigate the electric fields in arcs and Geissler tube discharges.

REFERENCES

[1] Fabry and Perot: *Ann. d. Chim. et Phys.* (7), **12**, 459, 1897.
[2] Herschel: *Phil. Trans.*, **99**, 274, 1809.
[3] Lummer: *Sitz. Berl. Acad.*, **24**, 504, 1900; *see also* No. 14.
[4] Moll: *Proc. Phys. Soc.*, **33**, 207, 1921.
[5] Childs: *Journ. Sci. Instruments*, **3**, 97, 129, 1926.
[6] Benoit: *Journ. de Phys.* (3), **7**, 57, 1898.
[7] Meggers: *Journ. Optical Soc. Amer.*, **5**, 308, 1921.
[8] Meggers and Peters: *Bull. Bur. Standards*, **14**, 697, 1918.
[9] Benoit, Fabry and Perot: *Trav. et mém. Bur. international*, Vol. 11, 1913.
[10] Perot and Fabry: *Ann. d. Chim. et Phys.* (7), **16**, 289, 1899.
[11] Perot and Fabry: *Ann. d. Chim. et Phys.* (7), **16**, 331, 1899.
[12] Houston: *Phys. Rev.*, **29**, 478, 1927.
[13] Gehrcke and Lau: D.R. Patent, No. **455553**, Cl. 42h, Group 20 (1927).
[14] Lummer: *Verh. Deutsch. Phys. Ges.*, **3**, 85, 1901.
[15] Lummer and Gehrcke: *Ann. der Phys.*, **10**, 457 (1903).
[16] Von Bayer: *Phys. Zeitschr.*, **9**, 831, 1908.
[17] A detailed analysis of both parallel and wedge plates has been given by Koláček, *Ann. der Phys.*, **39**, 1431 (1912).
[18] Fizeau and Foucault: *Ann. d. Chim. et Phys.* (3), **30**, 146, 1850.
[19] Esselbach: *Pogg. Ann.*, **98**, 513, 1856.
[20] Edser and Butler: *Phil. Mag.*, **46**, p. 207, 1898.
[21] Gehrcke and Reichenheim: *Verh. Deutsch. Phys. Ges.*, **4**, 209, 1906.
[22] Burns and Meggers: *Publ. Allegheny Obs.*, **6**, 109, 1925.
[23] Buisson, Fabry and Bourget: *Astro. Journ.*, **40**, 257, 1914.
[24] Williams: *Zeitschr. für Physik Bd.*, **53**, 542, 1929.

Printed in Great Britain by Butler & Tanner Ltd., Frome and London

HIGH VOLTAGE PHYSICS
By L. JACOB, M.Sc., A.R.C.Sc.I. (3s. 6d. net)

RELATIVITY PHYSICS
By W. H. McCREA, Ph.D., F.R.S.E.

FINE STRUCTURE IN LINE SPECTRA AND NUCLEAR SPIN
By S. TOLANSKY, B.Sc., Ph.D., A.Inst.P., D.I.C. (3s. 6d. net)

INFRA-RED AND RAMAN SPECTRA
By G. B. B. M. SUTHERLAND, M.A., Ph.D. (3s. 6d. net)

THERMIONIC EMISSION
By T. J. JONES, M.Sc. (3s. 6d. net)

ELECTRON DIFFRACTION
By R. BEECHING, A.R.C.S., B.Sc. (3s. 6d. net)

MAGNETISM
By EDMUND C. STONER, Ph.D. *New Edition, entirely Revised.* (3s. 6d. net)

THE EARTH'S MAGNETISM
By S. CHAPMAN, M.A., D.Sc., Vict.F.R.S. (4s. net)

MERCURY ARCS
By F. J. TEAGO, D.Sc., and J. F. GILL, M.Sc. (3s. 6d. net)

MOLECULAR BEAMS
By R. G. J. FRASER, Ph.D.

ALTERNATING CURRENT MEASUREMENTS
By DAVID OWEN, B.A., D.Sc., F.Inst.P. (4s. net)

COSMOLOGICAL THEORY
By G. C. McVITTIE, M.A.

DIPOLE MOMENTS
By R. J. W. LE FÈVRE, D.Sc., Ph.D. (4s. net)

FLUORESCENCE AND PHOSPHORESCENCE
By E. HIRSCHLAFF, Ph.D. (4s. net)

INTRODUCTION TO VECTOR ANALYSIS
By B. HAGUE, D.Sc. (3s. 6d. net)

THE CYCLOTRON
By W. B. MANN

THE SPECIAL THEORY OF RELATIVITY
By HERBERT DINGLE. (3s. 6d. net)

METHUEN'S MONOGRAPHS ON PHYSICAL SUBJECTS

SPECTRA. By R. C. JOHNSON, D.Sc. *Second Edition, Revised.*

WAVE MECHANICS. By H. T. FLINT, D.Sc., Ph.D. *Third Edition.* (4s. net)

THE PHYSICAL PRINCIPLES OF WIRELESS. By J. A. RATCLIFFE, M.A. *Fourth Edition.* (4s. net)

THE CONDUCTION OF ELECTRICITY THROUGH GASES. By K. G. EMELÉUS, M.A., Ph.D. *Second Edition.*

X-RAY CRYSTALLOGRAPHY. By R. W. JAMES, M.A., B.Sc.

THE COMMUTATOR MOTOR. By F. J. TEAGO, D.Sc.

APPLICATIONS OF INTERFEROMETRY. By W. EWART WILLIAMS, M.Sc. *Second Edition, Revised.*

THERMIONIC VACUUM TUBES. By E. V. APPLETON, M.A., D.Sc. F.R.S. *Third Edition, Revised.* (3s. 6d. net.)

PHOTOCHEMISTRY. By D. W. G. STYLE, B.Sc., Ph.D.

THERMODYNAMICS. By A. W. PORTER, D.Sc., F.R.S.

WIRELESS RECEIVERS. By C. W. OATLEY, M.A., D.Sc. *Second Edition.*

ATMOSPHERIC ELECTRICITY. By B. F. J. SCHONLAND, O.B.E., M.A., Ph.D.

THE METHOD OF DIMENSIONS. By A. W. PORTER, D.Sc.

COLLISION PROCESSES IN GASES. By F. L. ARNOT, B.Sc., Ph.D. (Camb.). (3s. 6d. net)

PHYSICAL CONSTANTS. Selected for Students by W. H. J. CHILDS, B.Sc., Ph.D. *Second Edition.*

ELECTROMAGNETIC WAVES. By F. W. G. WHITE, M.Sc. (3s. 6d. net)

THE GENERAL PRINCIPLES OF QUANTUM THEORY. By G. TEMPLE, Ph.D., D.Sc. (3s. 6d. net)

THE KINETIC THEORY OF GASES: Some Modern Aspects. By Professor MARTIN KNUDSEN.

LOW TEMPERATURE PHYSICS. By L. C. JACKSON, M.Sc., Ph.D. (3s. 6d. net)

Continued on back flap